RESEARCH ARTICLE

VOLCANICA

Evaluating steady-state volcanism in Iceland, La Réunion, Hawai'i, and western Galápagos: connections with volcanic hazards and future perspectives

Federico Galetto *[α,β], Beatriz Asfora[γ], and Matthew E. Pritchard[α]

[α] Cornell University; Earth and Atmospheric Sciences Department; Ithaca, NY, USA.
[β] Istituto Nazionale di Geofisica e Vulcanologia – Osservatorio Nazionale Terremoti; Roma, Italy.
[γ] Cornell University; Sibley School of Mechanical and Aerospace Engineering; Ithaca, NY, USA.

Submitted: 2025-08-29 | Accepted: 2026-02-06 | Published: 2026-02-11

Editor: O. Chevrel | Typesetter: J. Farquharson

Abstract

Steady-state volcanoes and magmatic provinces erupt magmas at nearly constant rates over the course of decades. Here, we analyzed the reliability of steady-state volcanism and its relationship with volcanic hazard evaluation in terms of forecasting the erupted volume at four frequently erupting oceanic hotspots: Iceland, La Réunion, Hawai'i, and western Galápagos. Over decadal timespans, these hotspots show steady-state activity often characterized by shorter-term cycles with an initial decrease in eruption rates, followed by an increase that rebalances the erupted volumes with the expected ones, providing a rough estimation of the maximum expected erupted volume of these paroxysmal periods. Although rarer, we also observe the opposite behaviour, with the eruption of more magma than expected, followed by low-rate periods proportional to the excess erupted volume. Steady-state rates can change over time, and future studies should investigate if these changes are related to longer-term episodes.

Riassunto

I vulcani e le provincie magmatiche in regime di stato stazionario eruttano magma a tassi quasi costanti nel corso delle decadi. Qui analizziamo l'affidabilità del vulcanismo in stato stazionario e la sua relazione con la valutazione del rischio vulcanico in termini di previsione dei volumi eruttati in quattro punti caldi oceanici che eruttano frequentemente: Islanda, La Réunion, Hawai'i e le Galápagos occidentali. Su scale di tempo decennali, questi punti caldi mostrano un'attività di stato stazionario spesso caratterizzata da cicli di breve periodo con un'iniziale decrescita nei tassi eruttivi seguita da una loro successiva crescita che ribilancia i volumi eruttati con quelli aspettati, fornendo una stima grezza del massimo volume eruttabile aspettato durante questi periodi parossistici. Sebbene sia più raro, abbiamo osservato anche il comportamento opposto, con l'eruzione di più magma di quello aspettato dai tassi stazionari, seguito da un periodo con bassi tassi eruttivi la cui durata è proporzionale al volume in eccesso eruttato. I tassi stazionari possono cambiare nel tempo e studi futuri dovrebbero investigare se questi cambiamenti possano essere collegati a episodi su scale temporali maggiori.

Keywords: Steady-state volcanism; Hot spots; Iceland; Galápagos; La Réunion; Hawai'i.

1 Introduction

G. Wadge introduced the concept of steady-state volcanism at the beginning of the 1980s for volcanoes that erupted magma at constant average rates over many years [Wadge 1980; Wadge and Guest 1981; Wadge 1982]. The steady-state activity of a volcano can therefore be identified by constructing the curve of cumulative volumes of erupted magma over time [Wadge 1982]. Figure 1 shows the different types of behaviour observed in steady-state volcanoes, as reported by Wadge [1982]. Type I (Figure 1) is characterized by continuous eruption rates matching with the steady-state rates. More often, steady-state volcanism shows fluctuations in the activity, which can be divided in three types (II–IV; Figure 1; Wadge [1982]). In type II, a series of eruptions with intervening repose periods generate a step-shaped curve, where a characteristic volume range defines the limits of the maximum erupted volumes and repose periods in this stage. Graphically, these limits are represented by two lines parallel to the average steady-state rate that envelope the step-shaped curve (Figure 1). Eruptions with volume significantly higher than that expected by the steady-state rates can be either followed (type III; Figure 1) or preceded (type IV; Figure 1) by repose periods (or periods with very low eruptive rates), whose duration is proportional to the volume erupted by these eruptions in order to rebalancing the real erupted volumes with those expected by the steady-state rates. Furthermore, Wadge [1982] reported that the steady-state activity can be interrupted by long-periods (also centuries) of quiescence not followed by large volume eruptions, but from a resumption of the steady-state volcanism at the same or different rates. The opposite, which is a large volume eruption not followed by a proportional period of quiescence but just by renewed activity at the previous steady-state rates, is rarer [Wadge 1982]. Thus, the activity of type III–IV shows a short-term (usually some years) change in the eruptive rates that can mask the steady-state characteristic of equilibrium between the expected and the erupted volumes. However, by looking at the cumulative erupted volumes over decades, it becomes evident how with the end of a type III or IV cycle the equilibrium between the expected and the erupted volumes come back to be confirmed, supporting the steady-state activity, as observed in all volca-

* federico.galetto@ingv.it

noes and magmatic provinces where steady-state activity has been identified.

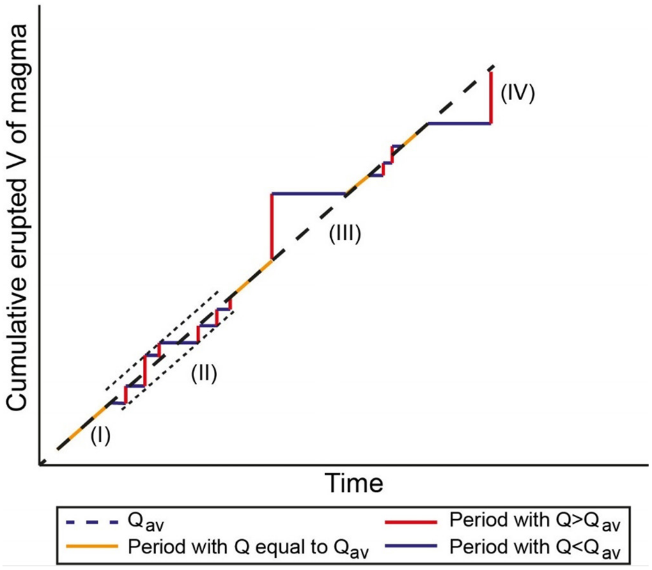

Figure 1: Schematic illustration of the main types (I–IV) of behaviour of the steady-state activity [based on Wadge 1982]. For a detailed description of the types I–IV of behaviour see the beginning of the introduction. The black dashed line represents the average steady-state rate (Q_{av}), while the orange, blue and red lines the cumulative volumes erupted over time (thus the observed eruptive rates Q). See Introduction for further details.

Different volcanoes have shown steady-state activity, such as Mt. Etna (Italy), Piton de la Fournaise (La Réunion, France), Nyamuragira (Democratic Republic of Congo), Kīlauea (USA), Klyuchevskoy and Bezymianny (Russia), and Santiaguito (Guatemala) [e.g. Wadge 1982; Bonaccorso and Calvari 2013; Coppola et al. 2021]. Ever since the theory of steady-state volcanism was first proposed, it has been observed that steady-state activity can be ascertained at different timescales (from decades to tens of kiloyears) and at both the scale of the single volcano and at the scale of the whole magmatic province [Wadge 1982; Kuntz et al. 1986; King 1989; Singer et al. 1997; Lipman 2000; Singer et al. 2008; Marturano et al. 2018; Yamamoto et al. 2018]. Steady-state activity has been ascertained in volcanoes and magmatic provinces with different magmatic composition and located in different tectonic settings, although steady-state activity occurring on timescales of few decades is mainly related to mafic and intermediate-composition volcanoes that more easily maintain sustained volcanic activity over many years [Wadge 1982; Crisp 1984; Kuntz et al. 1986; King 1989; Bonaccorso and Calvari 2013; Marturano et al. 2018; Yamamoto et al. 2018]. The causes of the steady-state volcanism are still debated, can differ from one province to another, and might be related to multiple processes acting together at different scales, from the geodynamic scale to the local scale [Wadge 1982; Crisp 1984]. Despite this, steady-state volcanism has implications for the evaluation of volcanic hazard, since it is one of the few tools available to provide a raw estimation of the maximum expected erupted volume at the onset of an eruption (types I, II, and IV; Figure 1) or, for an activity of type III (Figure 1), the duration of repose periods [Wadge 1982; King 1989; Bonaccorso and Calvari 2013; Calvari and Nunnari 2022]. In this frame, type IV is significant since it provides the maximum volume that can be erupted by paroxysmal periods following longer repose times (or times with low eruption rates), as done multiple times at Mt. Etna (Figure 2), although it is not possible to forecast the time of onset of the paroxysm [Wadge and Guest 1981; Wadge 1982; Harris et al. 2011; Bonaccorso and Calvari 2013; Calvari et al. 2020; Calvari and Nunnari 2022]. Type IV behaviour has been called size-predictable, while type III behaviour is time-predictable [e.g. De la Cruz-Reyna 1991; Bebbington 2014]. Thus, a better understanding of steady-state volcanism, and of how common types IV and III are, has implications for volcanic hazard evaluation, particularly the challenging problem of forecasting eruption size [Bebbington 2014].

Despite advances in methods of evaluating erupted volumes, steady-state activity has not been deeply analysed and investigated in the last couple of decades, especially in the context of magmatic provinces. Thus, to increase the knowledge on steady-state volcanism, here we investigated steady-state activity in four frequently erupting and well-studied oceanic hotspots (Iceland, La Réunion, Hawaiʻi, and western Galápagos). In two of them (Iceland and western Galápagos) volcanism is widespread, and we consider the volumes erupted by all their volcanoes to see if the steady-state activity exists at the level of the magmatic province, reflecting a possible steady-state regime of the hotspot. In the other two hotspots (Hawaiʻi and La Réunion) volcanism is localized, and the steady-state regime was previously identified [e.g. King 1989; Staudacher et al. 2016]. These four hotspots provide ideal case studies to investigate the steady-state volcanism since they erupt frequently and have constrained erupted volumes for many decades, allowing us to build curves of cumulative erupted volume for long periods. Furthermore, here we can also investigate the relationship between the present steady-state rates and the longer-term (≥10^3 yr) rates. Steady-state rates can provide an estimation of the maximum expected erupted volume [Wadge 1982; Bonaccorso and Calvari 2013; Calvari and Nunnari 2022], and we used two simple methods to quantify how well steady-state rates hindcast the erupted bulk volumes of each eruption, providing an estimation of the difference between the true erupted volume of each eruption and the expected maximum erupted volume from steady-state rates. When possible, we also included the volume of magma that remained intruded into the propagating dikes and sills to understand if some decrease in the observed erupted volumes can be related to higher intruded volumes.

2 Methodology

2.1 Dataset building

The erupted bulk and Dense Rock Equivalent (DRE) volume of magma come from previously published data (the list of these references is provided in the data availability statement and in Galetto [2026] Tables S1–S4). In Galetto [2026] Tables S1–S4 we also report the porosity assumed to convert the bulk volume to DRE (and vice versa) used by the published articles,

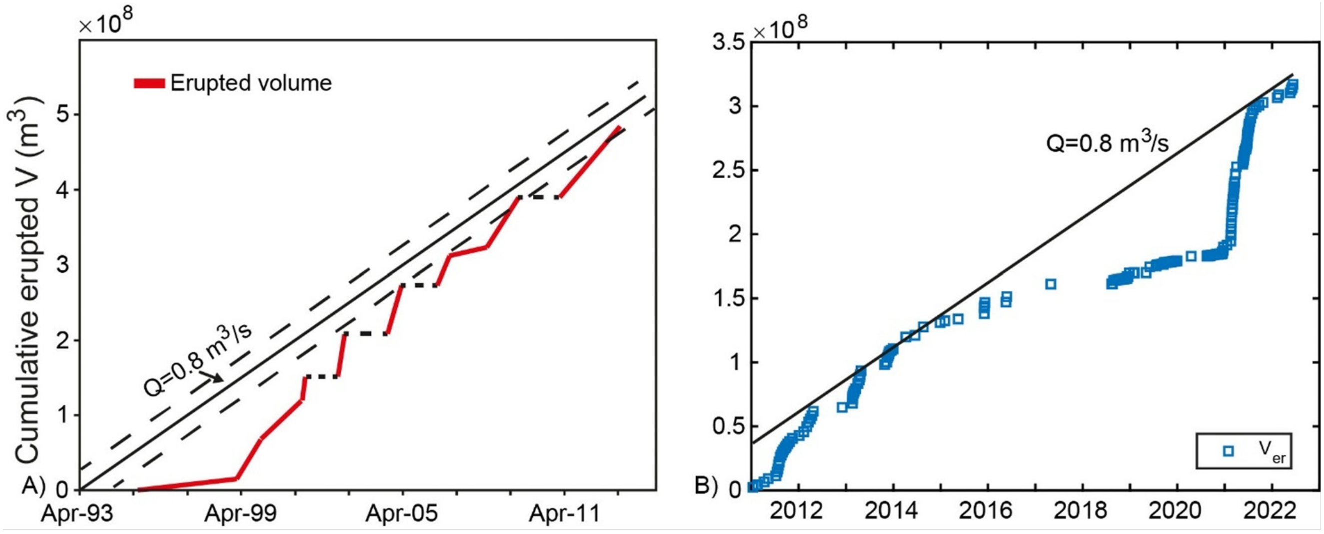

Figure 2: Example of the well-constrained steady-state activity at Mt. Etna (Italy) from 1993 to 2013 ([A] modified from Bonaccorso and Calvari [2013]) and from 2011 to 2022 ([B]; data from Calvari and Nunnari [2022]). The steady-state activity at Etna started since 1971 at constant rates of ~0.8 m^3 s^{-1} (back line). Dashed lines in [A] represent the uncertainties (standard deviation) associated with the steady-state rates [Bonaccorso and Calvari 2013, see].

as well as the one that we used for these conversions for the cases where previously published articles reported only the bulk or the DRE volume. In Galetto [2026] Text S1 and Figure S1, we report how we estimate the volumes of the 1979 and the 2008 eruptions at Cerro Azul (Galápagos), not available in previously published data. The dataset shows the erupted volumes up to 2023, with the exceptions of Iceland and western Galápagos for which we found also the volumes erupted in 2024.

Although the primary aim of this work is the analysis of steady-state volcanism, and thus of the erupted volumes, when possible we also reported the intruded volumes. However, in most cases these datasets are incomplete and thus we use this information just to identify possible relationship between reductions in the eruptive rates and increase in the intruded volumes for some periods. The intruded volume here is meant as the volume intruded into dikes and sills propagating outside the magma chamber during eruptions or intrusive events, and not as the volume of magma accumulated into the magma chamber in the inter-eruptive periods. The intrusive volumes here considered come from the inversion of geodetic data using elastic models and thus are considered as DRE volume [Chadwick et al. 2011; Wauthier et al. 2015; see also Galetto 2026] Text S2]. As for Hawai'i, which is characterized by a complex intrusive history analysed by previous studies [Dzurisin et al. 1984; Dvorak and Dzurisin 1993; Poland et al. 2014; Wright and Klein 2014; Montgomery-Brown and Miklius 2020], we do not report the intruded volumes, since it would require a detailed analysis that is beyond the aims of this work. However, we discuss how the observed steady-state rates at Hawai'i are affected by the intruded volumes, based on the results of the previous studies about intruded volumes at Hawai'i [Dzurisin et al. 1984; Dvorak and Dzurisin 1993; Poland et al. 2014; Wright and Klein 2014; Montgomery-Brown and Miklius 2020].

2.2 Steady-state volume prediction and statistical tests.

We applied two methods to evaluate the ability of steady-state rates to hindcast, and potentially forecast, the erupted bulk volumes (which are the better constrained volumes) of the four analysed hotspots during the studied time periods. The average steady-state rate (Q) is computed from the time series of cumulative volumes as (Equation 1):

$$Q = \frac{\Delta t}{\Delta V} \tag{1}$$

where Δt is the total timespan of the analysed period, and ΔV is the total cumulative volume erupted within this time. The rates for the four analysed hotspots are reported in Figures 3–6.

The first method, hereafter referred to as the Q-line fitting method, employs the average steady-state rate (Q) from Equation 1 to linearly extrapolate the expected cumulative bulk volumes over a given period. The difference between the hindcasted and observed values quantifies the error, which is graphically represented by the distance (along the y-axis direction) from the Q-line to the observed data (see Figure 7). The second approach, referred to as the deterministic time interval method, is based on the following linear state equation, obtained by rearranging Equation 1:

$$V_2 = Q(t_2 - t_1) + V_1 \tag{2}$$

where Q is the average steady-state rate of the studied period (from Equation 1), and V_1, V_2 are the cumulative bulk volumes after the eruptions that ended by time t_1 and t_2, respectively (see also Galetto [2026] Text S3 for La Réunion). By knowing Q, V_1, and the time interval between t_1 and t_2 for the eruptions in our dataset, it is possible to hindcast the cumulative volume V_2 resulting from the eruption that ends by time t_2. The error is again given by the difference between the calculated and observed cumulative volumes (see Figure 8). For both methods, we show the following error metrics: mean, standard deviation, and distribution (as a discrete histogram). The mean error quantifies systematic bias in the estimates, while the standard deviation quantifies the variability of the error across samples. The error distribution characterizes the shape and spread of the errors beyond what is captured by aggregate metrics, enabling evaluation of symmetry, tail behaviours, and the presence of outliers. Additional computed parameters and individual estimates are included in Galetto [2026] Text S4 and Tables S5–S6.

3 Steady-state hotspots results

3.1 Hot spots with widespread volcanism

3.1.1 *Iceland*

In Figures 3A–3B, we show the cumulative bulk (Figure 3A) and DRE (Figure 3B) volume of magma erupted in Iceland from 1961 (Askja eruption) to December 2024. These volumes have been compared with the longer-term average eruptive rates (bulk and DRE) estimated for about the last millennium in Iceland by Thordarson and Larsen [2007] (Figures 3A–3B). We observe that over the decadal analysed timespan, there is an overall good relation between the erupted volumes and the longer-term eruptive rates, although the cumulative erupted volume over time often shows type IV steady-state activity, with periods characterized by rates lower than the average, followed by periods with eruptive rates higher than the average that recover most (or all) of the volume not erupted in the periods with lower rates (Figures 3A–3B). A type IV cycle here in Iceland can last also for decades. For example, we observe that the 2011 eruptions at Eyjafjallajökull and Grímsvötn and the 2014–2015 Bárðarbunga eruption followed a long period characterized by rates lower than the average and re-equilibrated the cumulative erupted volumes of Iceland with the ones expected from the longer-term rates (Figures 3A–3B). The Bárðarbunga eruption was followed by years with rates lower than the average, with the Fagradalsfjall and Sundhnúkur eruptions that up to November 2024 have not yet re-equilibrated the cumulative erupted volumes of Iceland with the ones expected from longer-term rates, suggesting that Iceland might still be in a type IV cycle. Indeed, the total average bulk and DRE eruptive rates from 1961 to November 2024 are of ~0.102 $km^3\,yr^{-1}$ and of ~0.069 $km^3\,yr^{-1}$, respectively, which are slightly lower than the average longer-term bulk and DRE rates of ~0.111 $km^3\,yr^{-1}$ and of ~0.079 $km^3\,yr^{-1}$ estimated by Thordarson and Larsen [2007] (Figure 3A–3B). Since volcanoes in Iceland are placed within well-developed rift zones [Thordarson and Larsen 2007], the propagation of magma often occurs through well-developed vertical dikes that do not necessary intercept the topography triggering an eruption, as occurred multiple times during the 1975-1984 eruptive cycle at Krafla and the 2023–2024 eruptive cycle at Sundhnúkur [Tryggvason 1984; Tryggvason 1986; Parks et al. 2025]. Thus, for the four cases (Krafla, Bárðarbunga, Fagradalsfjall and Sundhnúkur) where the intruded volumes are known, we added to the erupted volume also the volume intruded as dikes, regardless of whether the dike triggers the eruption or not (Figure 3C). The addition of the intruded volumes for these four periods reveals some interesting patterns. For example, during the Krafla eruption (1975-1984), the period 1975 - July 1980 is characterized by eruptive rates lower than the steady-state rates (Figure 3A–3B) because this period was dominated by intrusions [Tryggvason 1984]. By considering also the volumes intruded as dikes, type IV activity observed from 1975 to 1984 in the cumulative erupted volumes (Figure 3A–3B) becomes a type I–type II activity (Figure 3C). Furthermore, we observe that the type IV activity from November 2023 to November 2024 becomes more evident (Figure 3C) once we consider also the important volumes intruded as dikes during the Sundhnúkur intrusive-eruptive sequence [Parks et al. 2025]. Thus, although our dataset of intrusive volumes is incomplete, the available data suggest that the steady-state behaviour remains confirmed, and likely even more evident, by considering the erupted plus intruded volumes. Due to the incompleteness of the dataset of the intruded volumes, the average intruded plus erupted rates of ~0.1 $km^3\,yr^{-1}$ in Figure 3C is a lower estimation. Future studies should better constrain the erupted + intruded V at Iceland.

3.1.2 *Western Galápagos (Ecuador)*

The western Galápagos volcanoes of Isabela and Fernandina islands make up a distinct magmatic province with respect to the eastern Galápagos volcanoes [Geist et al. 2014; Harpp and Geist 2018]. Thus, in this analysis we consider only the volumes erupted at the western Galápagos volcanoes, which are the most active. Contrary to the other analysed hotspots, the erupted volumes at western Galápagos volcanoes are constrained only for the last decades (Figure 4; Galetto [2026] Table S2). Despite this, from 1988 to present, the cumulative erupted volume suggests that also the western Galápagos are experiencing steady-state activity, with some observed type IV behaviours, at rates of ~0.025 $km^3\,yr^{-1}$ (bulk volume; Figure 4A), equivalent to ~0.018 $km^3\,yr^{-1}$ DRE (Figure 4B). These rates are higher than the longer-term (10^3–10^5 yr) rates of 0.0086 ± 0.0018 $km^3\,yr^{-1}$ (Figure 4B), although these latter are not well-constrained [Geist et al. 1994; Reynolds et al. 1995; Geist 1996; Naumann and Geist 2000; Geist et al. 2005; Kurz et al. 2014; Galetto et al. 2023a]. Figures 4A–4B show a large jump in the erupted volume in 1980 due to the large 1979–1980 eruption at Sierra Negra. Without an accurate knowledge of the volume erupted at the western Galápagos volcanoes before 1979, and from 1980 to 1988, it is difficult to understand whether this eruption is related to type III or IV steady-state activity, or if it has been an out-of-trend event not connected with the steady-state behaviours. For the same reason, it is not possible to know if the 1979–1980 eruption at Sierra Negra also caused a change in the steady-state rates.

The volume that remains intruded in dikes (or lateral sills) during eruptions at Western Galápagos volcanoes is often significant, with some events that are also only intrusive [Bagnardi and Amelung 2012; Guo et al. 2019; Galetto et al. 2020; Galetto 2023; Galetto et al. 2023b]. Since 1995 the intruded volumes have been estimated for all eruptions, except for the eruptions at Cerro Azul in 1998, at Sierra Negra in 2005 and the last eruption at Fernandina in 2024 (Galetto [2026] Table S2). Figure 4C shows the total cumulative volumes of erupted

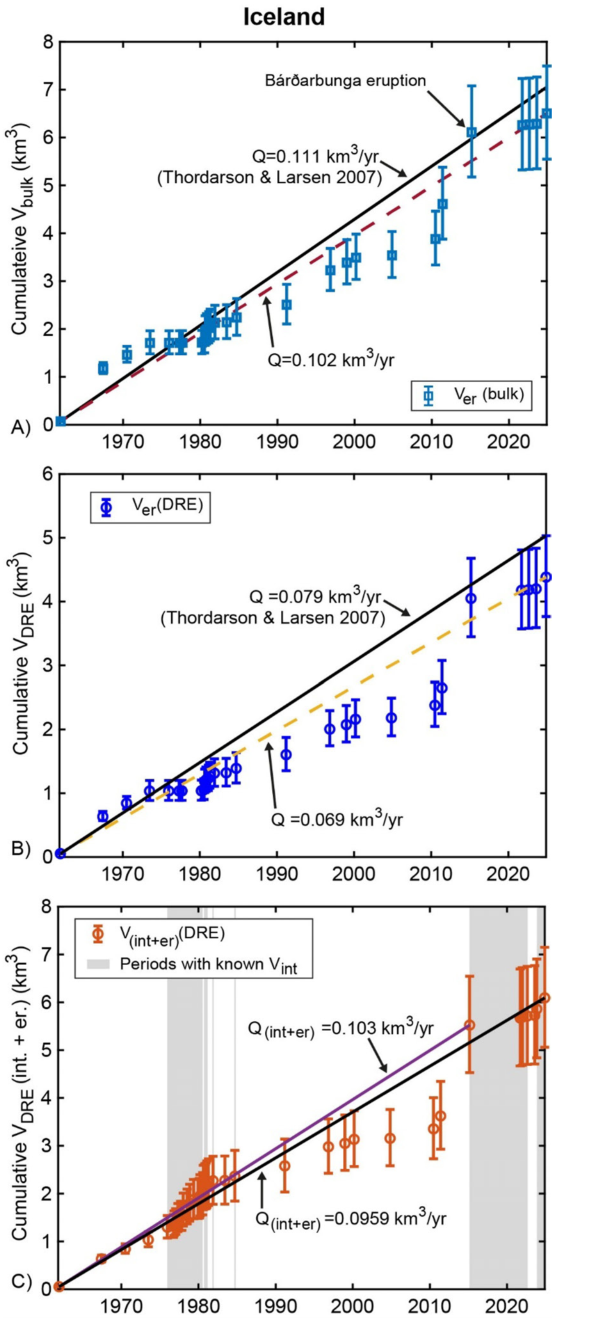

Figure 3: [A]–[B] Cumulative erupted bulk (panel [A]) and DRE (panel [B]) volumes of magma in Iceland. The black lines in panels are the average bulk (panel [A]) and DRE (panel [B]) eruption rates inferred by Thordarson and Larsen [2007] for about the last millennium. Red and yellow dashed lines in [A] and [B] are the average bulk and DRE eruption rates from 1961 to 2024, respectively. [C] Total cumulative volumes of erupted plus intruded (in the dikes) magma. The intruded volumes are constrained only for the periods within the grey areas. The violet and the black lines represent the average intrusive plus eruptive rates from 1961 to 2015 and from 1961 to 2024, respectively. These rates however are poorly constrained, since intruded volumes are known only for a few periods. Data and associated references are reported in Galetto [2026] Table S1.

plus intruded magma, with the steady-state activity that remains confirmed. Even in this case the calculated average extruded plus intruded rates of ~0.03 km^3 yr^{-1} are a minimum estimate due to the lack of three intruded volumes (Figure 4C).

3.2 Hotspots with localized volcanism

3.2.1 *La Réunion (Piton de la Fournaise)*

The magmatic activity at La Réunion is currently focused at Piton de la Fournaise volcano, which has a known steady-state activity [Wadge 1982; Staudacher et al. 2016; Vlastélic et al. 2018; Campus et al. 2025]. In Figure 5A–5C, we show the cumulative erupted bulk (Figure 5A–5B) and DRE (Figure 5C) volumes from 1931 to 2023 (data and references in Galetto [2026] Table S3). This long dataset allowed us to study two episodes of steady-state activity characterized by different steady-state rates: one from August 1936 to March 1998 and the second one from July 1999 to July 2023 (Figure 5A–5C). The first episode shows all types of activity (I–IV) of steady-state volcanoes (Figure 5A, 5C). In detail, we observe a few minor type III activities, connected for example with the December 1938 and the April 1961 eruptions (Figure 5A, 5C), and multiple type IV activities that became dominant especially during the period 1972-1982 that followed a period of six years of quiescence [Peltier et al. 2009]. We calculated average bulk steady-state rates of the first episode (1936-1998) of 0.011 km^3 yr^{-1} (Figure 5A). The corresponding DRE steady-state rates of the first episode are of 0.006 km^3 yr^{-1} (Figure 5C). The second episode is characterized by an increase in the average steady-state rates, well documented by previous studies [e.g. Peltier et al. 2009; Staudacher et al. 2016; Peltier et al. 2018; Vlastélic et al. 2018]. We calculated for the second episode bulk steady-state rates of 0.022 km^3 yr^{-1} from 1999 to 2023 (DRE rates of 0.013 km^3 yr^{-1}; Figure 5C) and of 0.023 km^3 yr^{-1} (0.014 km^3 yr^{-1} DRE) from 1999 to April 2020, which provides a slightly better fitting of the data (Figure 5B). The second episode is characterized by type III behaviour. Indeed, after about 9 years (July 1999-March 2007) of type I-II steady-state activity, an out of trend eruption occurred at the beginning of April 2007 (the caldera collapse eruption; Figure 5). This eruption, however, was followed by 7 years of eruptive rates significantly lower than the steady-state rates, leading to a re-equilibrium of the erupted volumes with those expected by the steady-state rates (type III behaviour, Figure 5). Then, the eruptive rates returned comparable to the steady-state rates (Figure 5). Piton de la Fournaise has also a dataset of the intruded volumes that allows to calculate the total intruded plus erupted DRE volumes up to December 2020 [Derrien 2019; Dumont et al. 2022, Figure 5C–5D]. The steady-state activity remains confirmed, with intruded plus erupted DRE rates of 0.008 km^3 yr^{-1} for the first episode and of 0.018 km^3 yr^{-1} for the second episode computed from 1999 to December 2020 (last date with well constrained intruded volume).

Finally, both episodes show steady-state rates higher than the long-term (2×10^6 yr) eruptive rates of 0.0024 km^3 yr^{-1} constrained by Gerlach [1990], and also reported in White et

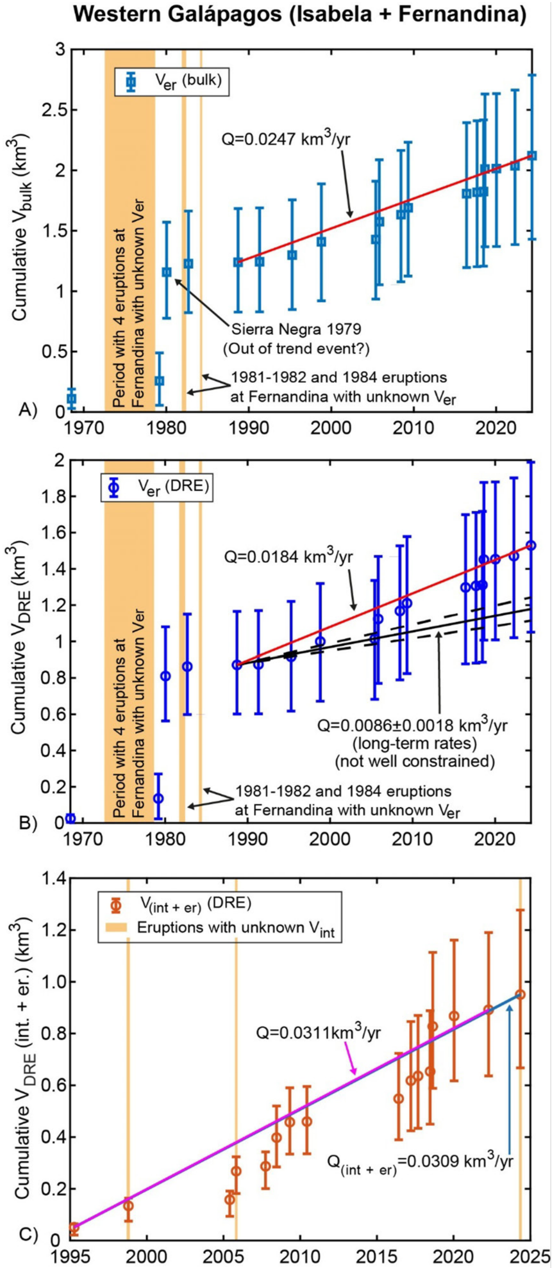

Figure 4: [A]–[B] Cumulative erupted bulk (panel [A]) and DRE (panel [B]) volume of magma from western Galápagos volcanoes. Red lines in [A] and [B] are the average bulk and DRE eruption rates from 1988 to 2024, respectively. The black lines in [B] represent the longer-term (10^3–10^5 yr) eruptive rates estimated for the western Galápagos by previous authors (see text in Section *3.1.2*). [C] Cumulative total volume (DRE) of magma erupted and intruded (as dikes) in western Galápagos. The blue and purple lines are the average intrusive plus eruptive rates estimated from 1995 to 2024 and from 1995 to 2022 (excluding the 2024 eruption at Fernandina with unknown intruded volumes), respectively. Data and associated references in Galetto [2026] Table S2.

al. [2006], which however are mainly based on an older dataset compiled from 1969 to 1972 [Gerlach 1990].

3.2.2 *Hawai'i (USA)*

The current hotspot volcanic activity in Hawaiʻi is focused at the volcanoes of Kīlauea and Mauna Loa. Steady-state activity in Hawaiʻi was previously identified from the 1920s to the 1980s [Dzurisin et al. 1984; King 1989; Dvorak and Dzurisin 1993]. Here we collected the volumes erupted in Hawaiʻi from 1903 to 2023, although some volumes erupted at Kīlauea from 1903 to 1918 are unknown (Figure 6). From 1993 to 2018, it has been more difficult to compile the year-by-year erupted volumes from available published data and therefore we just report the total volumes erupted during the time intervals defined by [Orr et al. 2015] and [Neal et al. 2019]. This fact, however, does not affect our results, since it still allows us to investigate the cumulative total erupted volumes that are the target of the analysis of the steady-state volcanism. The cumulative bulk (Figure 6A–6C) and DRE (Figure 6D) erupted volumes shows that the steady-state activity of Hawaiʻi can be divided in two main episodes: from August 1923 to the 1984 Mauna Loa eruption (Figure 6B) and from 1984 (after the Mauna Loa eruption) to 2023 (Figure 6C). The first episode was characterized mainly by consecutive events of type IV activity (Figure 6B). The predominance of type IV activity during this episode can be related also to the intruded volumes that have been important during some periods characterised by low eruptive rates, such as the 1977–1980 [see details in Dzurisin et al. 1984; Klein et al. 1987; Dvorak and Dzurisin 1993; Heliker and Mattox 2003; Wright and Klein 2014]. For the first episode, we calculated average bulk and DRE steady-state rates of 0.04 $km^3\,yr^{-1}$ and 0.03 $km^3\,yr^{-1}$, respectively (Figure 6). The first period ended in April 1984, with the volumes erupted by the onset of the 1983–2018 eruption at Kīlauea and with those erupted by the 1984 eruption at Mauna Loa. After the 1984 Mauna Loa eruption, the volume of extrusive material erupted at Hawaiʻi until 2018 was erupted continuously by Kīlauea volcano during the 1983–2018 eruption, characterized by average eruptive rates higher than those of the previous episode [Dvorak and Dzurisin 1993; Wright and Klein 2014; Orr et al. 2015]. We calculated for the second episode (1984–2023) average bulk and DRE steady-state rates of ~0.19 and ~0.14 $km^3\,yr^{-1}$, respectively (Figure 6). These rates are significantly higher than those of the first episode. However, a detailed analysis of the eruptive rates of the second episodes reveals further changes (Figure 6C). Indeed, the average bulk rates have been of ~0.13 $km^3\,yr^{-1}$ (~0.09 $km^3\,yr^{-1}$ DRE) up to 1993 and then increased from 1993 to December 2022 (~0.2 $km^3\,yr^{-1}$ bulk and ~0.15 $km^3\,yr^{-1}$ DRE). The rates slightly slowed down again in 2023, which might hint also to the beginning of a type IV activity or of a new episode. It is interesting to note that the 2018 eruption at Kīlauea shows behaviours of both type III and IV (Figure 6C). Indeed, this large eruption was preceded by a period with rates lower than the steady-state rates (type IV), but it erupted more magma than expected and was followed by a quiescent period proportional to the "excess" volume (type III). [Figure 6D; Lipman 1995; Quane et al. 2000]. Steady-state rates of the first and second episodes are respectively lower than, and nearly equal to, the combined long-term eruptive rates of Kīlauea and Mauna Loa (0.14 $km^3\,yr^{-1}$) reported by White et al. [2006] for the past

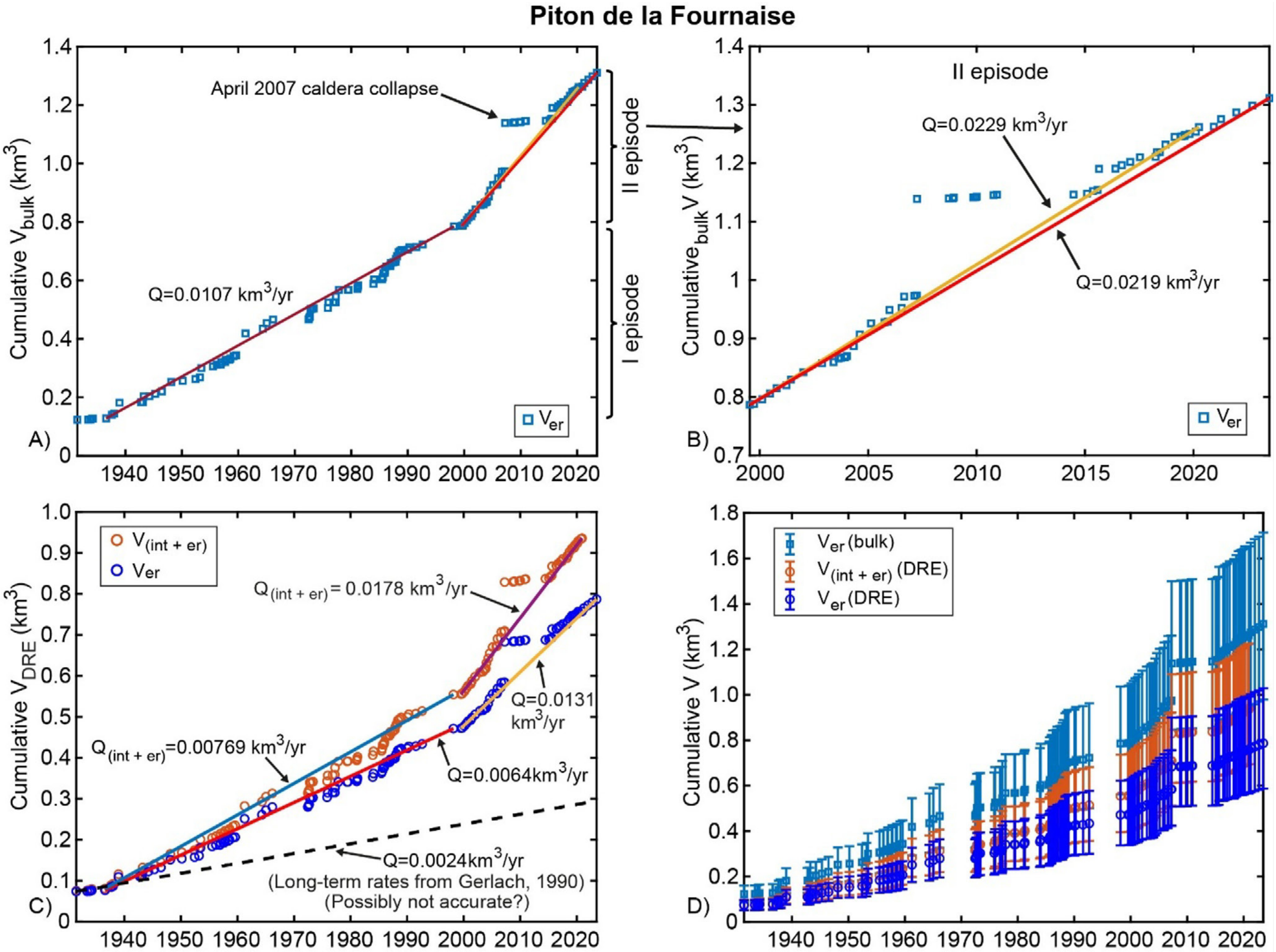

Figure 5: [A]–[B] Cumulative erupted bulk volumes of magma at Piton de la Fournaise (La Réunion). The dark red line in [A] represents the average rates 1931 to 1998, while the yellow and red lines (panels [A]–[B]) represent the average rates calculated from 1999 to April 2020 and from 1999 to 2023, respectively. [B] shows a zoom of the cumulative bulk volumes erupted during the II episode (1999-2023). [C] Cumulative DRE volumes of erupted magma (blue dots) and of intruded (int) plus erupted (er) volumes (orange dots). The red and yellow lines represent the average DRE steady-state rates from 1931 to 1998 and from 1999 to 2023, respectively. The blue and violet lines represent the average DRE intruded plus erupted rates from 1931 to 1998 and from 1999 to December 2020 (date with the last well constrained intruded volume), respectively. D) Errors associated with data in [A]–[C]. Data and associated references reported in Galetto [2026] Table S3.

0.4–0.5 million years (Figure 4C). They are respectively lower and higher than the combined eruptive rate of 0.07 $km^3\ yr^{-1}$ estimated for the past few thousand years [Figure 6D; Lipman 1995; Quane et al. 2000].

4 Steady-state cumulative bulk volume prediction results

Analysis of historical eruption data shows that individual bulk erupted volumes and the intervals between consecutive eruptions consistently display right-skew normal characteristics [O'Hagan and Leonard 1976], across all studied periods and hotspots (Galetto [2026] Figures S2–S6). This indicates that the data conform to a relatively well-behaved statistical distribution. Additionally, when considering the cumulative erupted volumes over time, the data align with fitting lines whose slopes correspond to the average steady-state rates (Figure 7–8), a pattern that is encouraging for predictive applications. Building on this empirical characterization, we applied the two methods described in Section 2.2 to evaluate their ability to predict cumulative bulk volumes from the steady-state equation. Galetto [2026] Table S5 reports the results obtained using both methods for each eruption, and Galetto [2026] Table S6 provides a comparison of error statistics for the two methods across the four analysed hotspots (see Galetto [2026] Text S4 for calculation details).

Figure 7 shows the results obtained with the Q-line fitting method (see Section 2.2, Equation 1). As expected, for each analysed hotspot this method yields lower errors (difference between the cumulative erupted and expected volumes) during type I and II activity, and higher errors during types III and IV activity, since they mark a shift from the linear behaviour (Figure 5; Galetto [2026] Tables S5–S6). Although the error between the expected and the erupted volume of an eruption

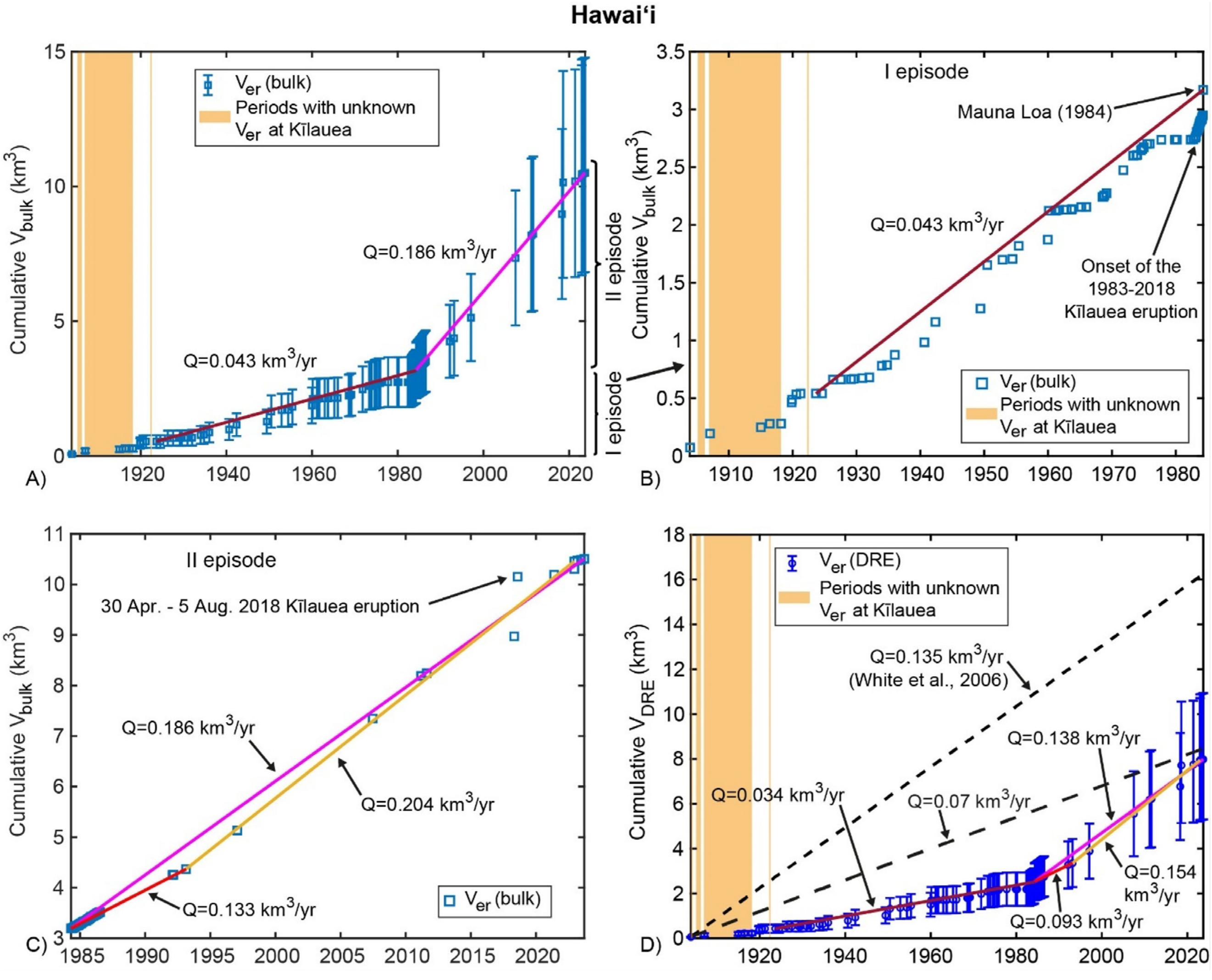

Figure 6: Cumulative bulk (panels [A]–[C]) and DRE (panel [D]) volumes of magma erupted in Hawai'i. [B] and [C] show a subset of the data in [A], with [B] showing the data from 1903 to the 1984 Mauna Loa eruption (thus including the I episode) and panel c data from 1984 (after the Mauna Loa eruption) to 2023 (II episode). Dark red and magenta lines are the average steady-state of the I (1923–1984) and II episode (1984–2023) respectively. Red and yellow lines show the average rates from 1984 to 1993 and from 1993 to 2022 respectively. Dashed lines in panel d are the eruptive rates reported in White et al. [2006] for the last millions of years (0.135 km^3 yr^{-1}) and in Lipman [1995] for the last kiloyears (0.07 km^3 yr^{-1}). Data and associated references in Galetto [2026] Table S4.

can be high during periods with activity of type III and IV, it is important to note that in all the analysed cases the error decreases again by the end of the corresponding type III or IV cycle (Figure 7B, 7E, 7H, 7K). This pattern is consistent with rebalancing of erupted volumes relative to steady-state rates over time.

When estimation errors arise from many independent random contributions and can therefore be viewed as the sum of multiple random variables, the central limit theorem predicts that their distribution approaches a Gaussian [Walker 1969]. Under this assumption, error distributions that more closely resemble a zero-mean Gaussian are commonly associated with better estimation performance. In this context, hotspots dominated by pronounced type IV activity (e.g. Iceland and the western Galápagos) exhibit error distributions with stronger deviations from a zero-mean Gaussian, including a higher prevalence of outliers (Figure 7C and 7F). By contrast systems with type I–II activity or type IV activity that often remains closer to the steady-state-rate (e.g. Piton de la Fournaise, Figure 7I) show error distributions closer to Gaussian behaviour, with more stable model performance.

Figure 8 shows results of the deterministic time interval method (see Section 2.2, Equation 2), which outperforms the previous method in forecasting cumulative erupted volumes (Figure 8 8; Galetto [2026] Table S5). Although periods associated with the largest departures from steady behaviour (points of maximum shift during type III–IV activity) still exhibit high errors (Figure 8), these are often lower than those encountered with the Q-line fitting method (Figure 7–8; Galetto [2026] Table S5). Overall, the error distribution for all analysed

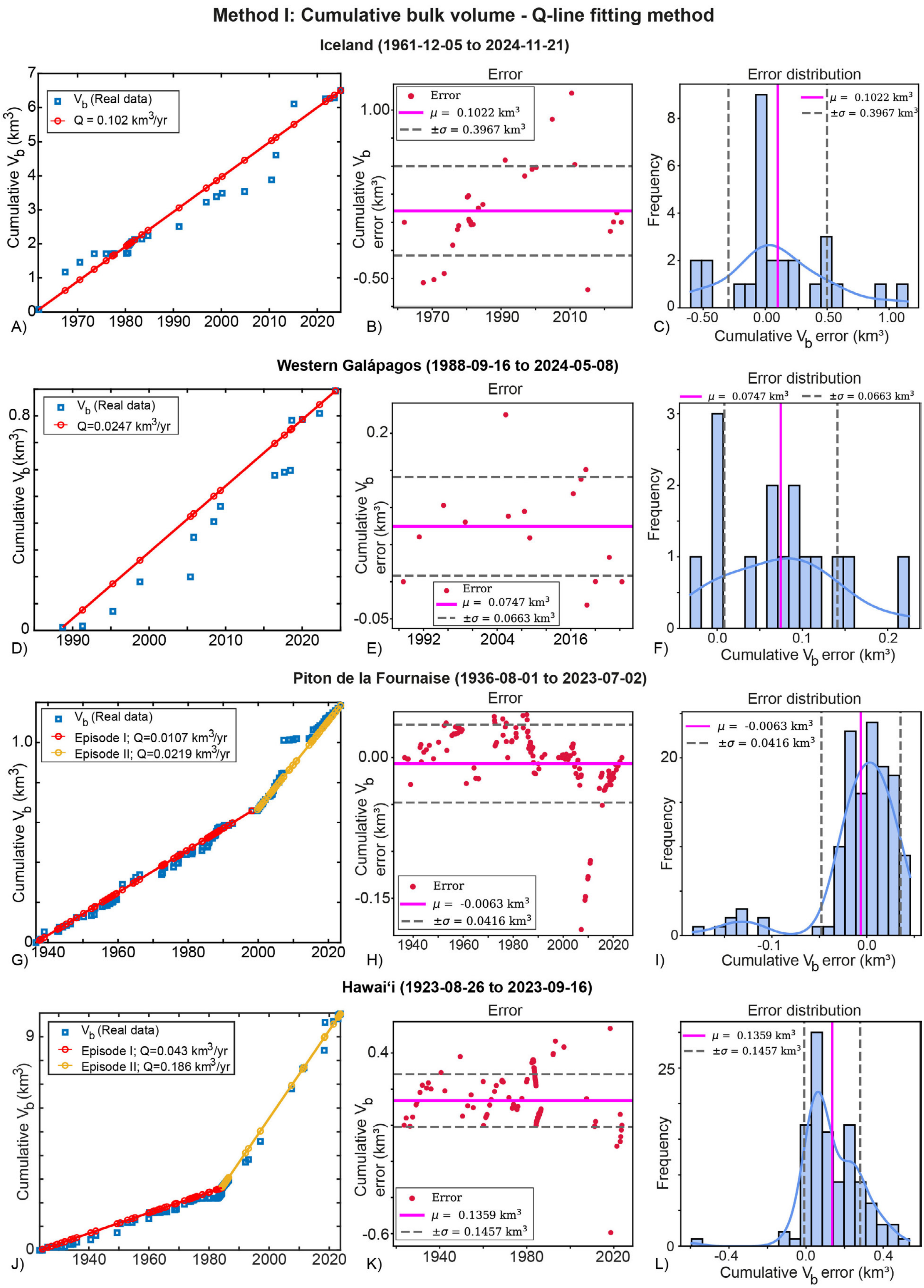

Figure 7: [A], [D], [G], [J] Expected cumulative bulk volumes (red and orange dots) obtained with the *Q*-line fitting method (method I; Section 2.2). [B], [E], [H], [K] Associated errors (difference between the real data and the expected ones) and their frequency distribution (panels [C], [I], [F] ,[L]).

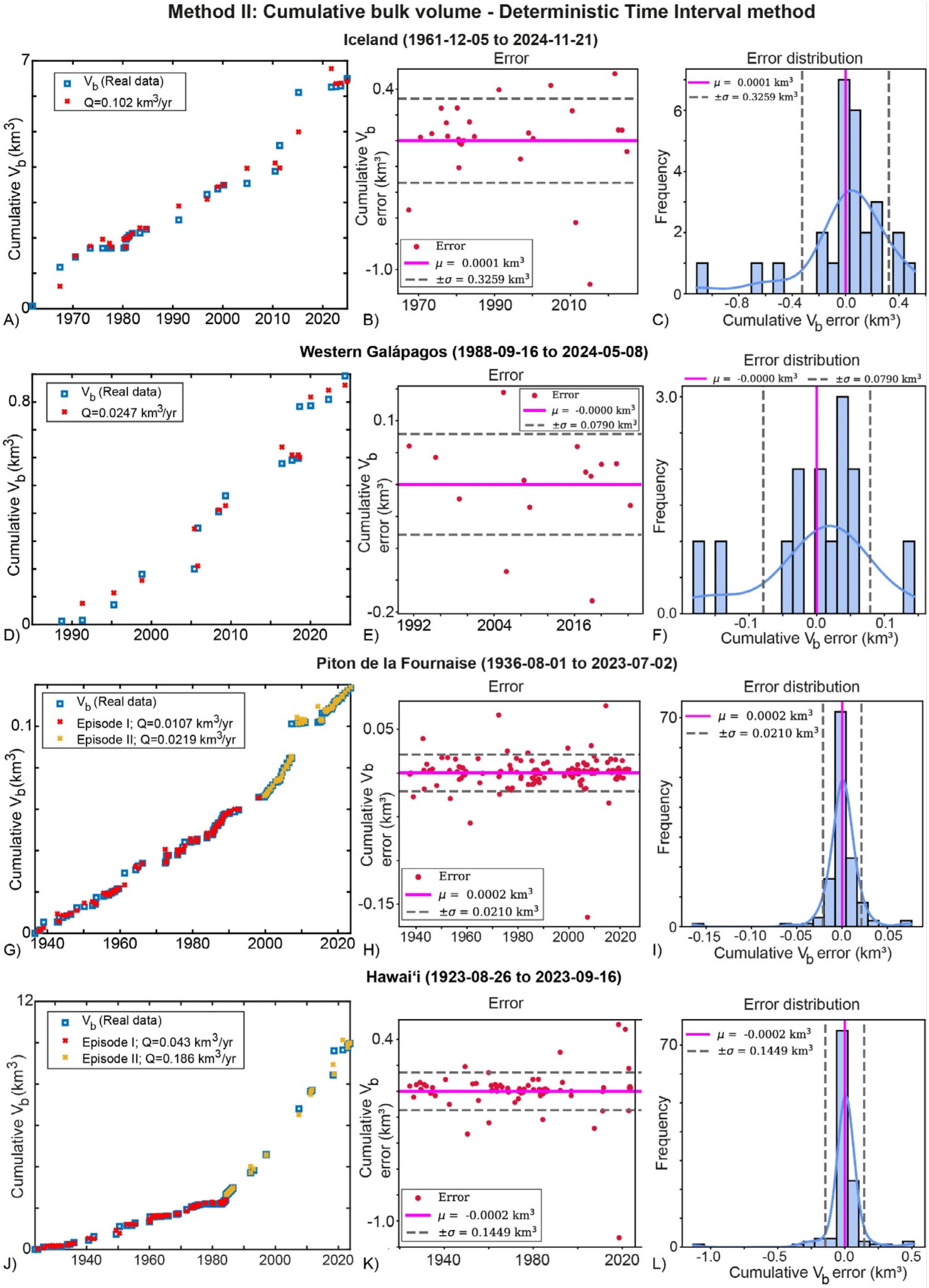

Figure 8: [A], [D], [G], [J] Expected cumulative bulk volumes (red and orange cross) obtained with deterministic time interval method (see Section 2.2). [B], [E], [H], [K] Associated errors (difference between the real data and the expected ones) and their frequency distribution (panels [C], [I], [F] ,[L]).

hotspots increasingly approaches a zero-mean Gaussian (Figure 8C, 8F, 8I, 8L), with some negative skewness caused by significant type III activity (e.g. Piton de la Fournaise, Figure 7I and 8I). When errors are normalized by the total cumulative erupted volume to account for differences the in total erupted volume among hotspots (Galetto [2026] Table S6), the estimation error in both methods increases in the following order: Hawai'i, Piton de la Fournaise, Iceland, and the western Galápagos (Galetto [2026] Table S6). Note that the method performance might also be influenced by differences in data availability across hotspots, with more extensive eruptive records for systems such as Hawai'i and Piton de la Fournaise (Galetto [2026] Table S6).

We also tested the two methods by using the rates computed for the second episode at La Réunion from 1999 to April 2020 (Figure 5B; Galetto [2026] Figure S7) and at Hawai'i by dividing the second episode in two parts (1988–1993 and 1993–December 2022; Figure 6C; Galetto [2026] Figure S8). Results show a decrease in the errors of the predicted volumes with the Q-line fitting method due to a better linear fitting by using the average rates constrained in these timespans, while the deterministic time interval method produced similar results (Galetto [2026] Figures S7–S8, Tables S5–S6).

5 Discussion

5.1 Steady-state volcanism and volcanic hazard

The four analysed oceanic hotspots (Iceland, La Réunion, Hawai'i, and western Galápagos), whose continuous or frequent volcanic activity is directly fed by mantle plumes, provide us ideal case studies to investigate steady-state volcanism in magmatic provinces. Our data show that the analysed hotspots are in a steady-state of activity, for which we calculated the bulk and DRE steady-state eruption rates. At La Réunion and Hawai'i the steady-state activity was previously identified [King 1989; Dvorak and Dzurisin 1993; Staudacher et al. 2016]. In detail, at La Réunion the calculated average bulk steady-state rates (0.011 $km^3\,yr^{-1}$) of the first episode (1936–1998) are consistent with the rates of 0.010 $km^3\,yr^{-1}$ calculated by Staudacher et al. [2016] for the period 1950–1998. On the contrary, for the second episode (1999–2023) we calculated bulk steady-state rates (0.02 $km^3\,yr^{-1}$) that are lower than the 0.03 $km^3\,yr^{-1}$ estimated by Staudacher et al. [2016] for the period 1998–2013. This discrepancy is however mainly due to: 1) the fact that the volumes erupted in the large April 2007 eruption have been re-estimated (and lowered) after Staudacher et al. [2016] [Peltier et al. 2018; Derrien 2019] and 2) in 2013 the cycle with type III activity connected to the April 2007 eruption was not ended yet and thus the cumulative erupted volumes were still higher than those expected by the steady-state rates that can be computed before the onset of this type III activity (Figure 5). It is important to remember that the determination of the steady-state rates is indeed influenced by the arbitrary choice of the dates used to compute them [King 1989]. As for Hawai'i, the bulk steady-state rate (0.043 $km^3\,yr^{-1}$) of the first episode (1923–1984) is: 1) consistent with the rates of 0.04 $km^3\,yr^{-1}$ estimated by Macdonald et al. [1983] for the period 1919–1982; 2) higher than the rates of 0.036 $km^3\,yr^{-1}$ estimated by King [1989] for the period 1919–1984; 3) lower than 0.05 $km^3\,yr^{-1}$ for the period 1823–1969 calculated by Moore [1970]. The increase in the eruptive rates during the second episode was identified by previous studies, and is consistent with the studies from which we took the erupted volumes [Dvorak and Dzurisin 1993; Heliker and Mattox 2003; Poland et al. 2014; Orr et al. 2015; Neal et al. 2019; Dietterich et al. 2021; Mulliken et al. 2024].

The steady-state activity observed in these hotspots shows all the main behaviours (type I–IV) firstly proposed by Wadge [1982], with a predominance of type IV steady-state activity. The repeated occurrence of small (possible connected also with type II) or large type IV activity observed at all the analyzed hotspots suggest that the size of the next paroxysmic event is directly related to the time of the repose period (or of the period with rates significantly lower than the steady-state rates), as observed also at other steady-state volcanoes [Bonaccorso and Calvari 2013; Calvari and Nunnari 2022]. Thus, the larger the period with no eruption (or characterized by low eruptive rates), the higher the possibility to have larger eruptions, with important implications in the evaluation of the volcanic hazard of these hotspots. Although type IV behaviour does not allow one to forecast the time of onset of the eruption(s) that will re-equilibrate the erupted volumes, it provides an empirical tool for forecasting the maximum size of the expected eruptions after longer repose periods [Bonaccorso and Calvari 2013; Calvari and Nunnari 2022]. Our data show that a type IV cycle can last also for a decade or more (e.g. Iceland and Hawai'i) and that the re-equilibrium can occur through multiple eruptions. For example, in Iceland the re-equilibration after the low eruptive rates that characterized the first decade of this millennium occurred in five years through three eruptions (the 2011 eruptions at Eyjafjallajökull and Grímsvötn and the 2014–2015 Bárðarbunga; Figure 3A). This is consistent with what was observed multiple times at Mt. Etna [Figure 2; Bonaccorso and Calvari 2013; Calvari and Nunnari 2022]. The fact that the re-equilibrium between the true and the expected cumulative erupted volumes can also occur through multiple eruptions has implications for the evaluation of the volcanic hazard, since if a paroxysmic eruption does not completely re-equilibrate the erupted with the expected volumes, it is possible that future paroxysmic eruption(s) will occur to complete the re-equilibrium. For example, in Iceland the Bárðarbunga eruption was followed by years with rates lower than the average, so that the total average bulk and DRE eruptive rates from 1961 to November 2024 are of ~0.102 $km^3\,yr^{-1}$ and of ~0.069 $km^3\,yr^{-1}$, respectively, which are slightly lower than the average longer-term bulk and DRE rates of ~0.111 $km^3\,yr^{-1}$ and of ~0.079 $km^3\,yr^{-1}$ estimated by Thordarson and Larsen [2007] (Figure 3A–3B). This hints to the possibility that Iceland in November 2024 was still not in equilibrium with the expected erupted volumes from the average rates in Thordarson and Larsen [2007], potentially explaining why Iceland erupted again in 2025.

In our datasets, type III activity is much rarer than type IV. Type III activity does not allow forecasting the expected erupted volume of the paroxysm but is however equally important since it hints to a period of no, or small, volcanic activity after the paroxysm proportional to the erupted volume [Wadge 1982]. The type I–IV behaviours have been observed in many other steady-state volcanoes and magmatic provinces, with Nyamuragira and Mt. Etna providing the other two well-studied examples of steady-state activity constrained over >50 years [Wadge 1982; Bonaccorso and Calvari 2013; Yamamoto et al. 2018; Burgi et al. 2021; Coppola et al. 2021; Pouclet and Bram 2021; Calvari and Nunnari 2022]. Finally, we found the 2018 eruption at Kīlauea shows a mixed behaviour of type IV–III activity.

The occurrence of type III and IV activity, as well as the fact that the re-equilibration after type IV activity can occur with multiple eruptions over some years, complicates efforts to precisely forecast the size of each eruption. This is shown by the analysis in Section 4, where sometimes the predicted volumes show large errors, especially in the periods of maximum deviation from the linear behaviour during type III and IV (Galetto [2026] Tables S5–S6). Thus, steady-state volcanism does not always allow precise forecasting of the size of next eruption, but provides a powerful tool to obtain: 1) a raw estimation of the expected cumulative volumes over the decades; 2) the expected total volumes erupted by paroxysm periods (that can involve more than one eruption) in type IV activity; 3) the duration of the repose/low activity time in a type III activity. All these constitute valuable information for the evaluation of volcanic hazards. Furthermore, the Q-line fitting and the deterministic time interval methods were applied here in a hindcasting framework, using the known time intervals between eruptions. However, it might also be applied in a forecasting context by simulating different possible time intervals and evaluating the corresponding expected erupted volumes.

In this study we do not present a detailed analysis of the intruded plus erupted rates, since intruded volume are usually less well constrained and therefore the total (intruded + erupted) rates should be better investigated and constrained in future dedicated studies. However, some preliminary considerations can be done even from the dataset that we show in Figure 3–5 and from previously published analyses for Hawai'i [Poland et al. 2014] and for Kīlauea in particular, since here the intruded volumes are better constrained [Dzurisin et al. 1984; Dvorak and Dzurisin 1993; Wright and Klein 2014]. First, at Piton de la Fournaise and western Galápagos the steady-state characteristics remain confirmed even by adding the intruded volumes. For Iceland we have some substantial gaps in the intruded volumes, but an interesting aspect is that by considering only the erupted volumes, the 1975–1984 Krafla eruption shows type IV characteristics, while by considering also the intruded volumes it shows type I characteristics (Figure 3C). On the contrary, type IV behaviour becomes more evident (with a better re-equilibrium of the expected volumes) by considering also the intruded volumes during the 2023–2024 Sundhnúkur intrusive-eruptive sequence (Figure 3C). Also at Kīlauea, previous studies show that over many decades the cumulative curves of intruded plus erupted volumes exhibit some steady-state characteristics [Dzurisin et al. 1984; Dvorak and Dzurisin 1993]: some periods are characterized by type IV eruptive activity that becomes less pronounced after the inclusion of the intruded volumes (e.g. 1960–1965 [Dvorak and Dzurisin 1993]), while others maintain type IV characteristics, with an initial reduction in the total rates (lasting years) followed by an increase in the total rates [see Dzurisin et al. 1984; Dvorak and Dzurisin 1993; Poland et al. 2014; Wright and Klein 2014].

5.2 Changes in steady-state volcanism and its relationship to the long-term rates.

Hawai'i and Piton de la Fournaise show that the steady-state rates can change after many decades, starting a new episode (Figure 5 and 6), similar to what was observed for Nyamuragira and Etna [Harris et al. 2011; Pouclet and Bram 2021]. While at Etna the change in the steady-state rates from one episode to another one was characterized by changes in the composition, frequency, and main location of eruptions [Clocchiatti et al. 2004; Viccaro et al. 2011; Cappello et al. 2019; Di Renzo et al. 2019], Piton de la Fournaise and Hawai'i show more complex characteristics that shed light on the stability of the steady-state volcanism. Vlastélic et al. [2018] associated changes in the $^{87}Sr/^{86}Sr$ and incompatible trace elements ratios of erupted lavas at Piton de la Fournaise to changes in the fertility of the mantle source that fed the volcanism, and used these changes to divide the eruptive sequence of Piton de la Fournaise from 1942 to 2017 in four cycles. While the passage from cycle 2 to cycle 3 identified by Vlastélic et al. [2018] is consistent with the onset of the new episode characterized by higher steady-state rates, it is interesting to note how the transitions between the other cycles (especially between cycle 1 and 2) were not characterized by changes in the steady-state rates [Vlastélic et al. 2018]. Similar results have been found for Hawai'i, where the short term (usually <10–15 years) eruptive activity has been divided in different events characterized by changes in the composition, intrusive versus extrusive volume ratio, location of the eruptions, and magma supply [e.g. Dzurisin et al. 1984; Klein et al. 1987; Dvorak and Dzurisin 1993; Heliker and Mattox 2003; Poland et al. 2012; Greene et al. 2013; Poland et al. 2014; Wright and Klein 2014]. However, despite this variability on the short-term, the cumulative erupted volumes over decades shows a steady-state behaviour [King 1989, Figure 6,], with the change in the decadal steady-state rates correlated with the occurrence of the large 1983–2018 Kīlauea eruption [Heliker and Mattox 2003; Orr et al. 2015; Mulliken et al. 2024]. Thus, the case studies of Piton de la Fournaise and Hawai'i suggest that changes in the magmatic system do not always trigger a change in the decadal steady-state rates, although these changes can affect the type of observed behaviours (type I–IV) during the steady-state activity.

Future studies should also investigate whether changes in the decadal steady-state rates might be considered as step-changes in the longer-term (from centuries to millennia) steady-state activity or not. Indeed, at some volcanoes and magmatic provinces steady-state activity has been recognized at different timescales (from decades to tens of kiloyears), despite the challenges to map, date and quantify the volume of the old deposits [Wadge 1982; Civetta et al. 1988; Singer et al. 1997; Lipman 2000; Jicha and Singer 2006; Singer et al. 2008; Marturano et al. 2018; Yamamoto et al. 2018; Nasholds and

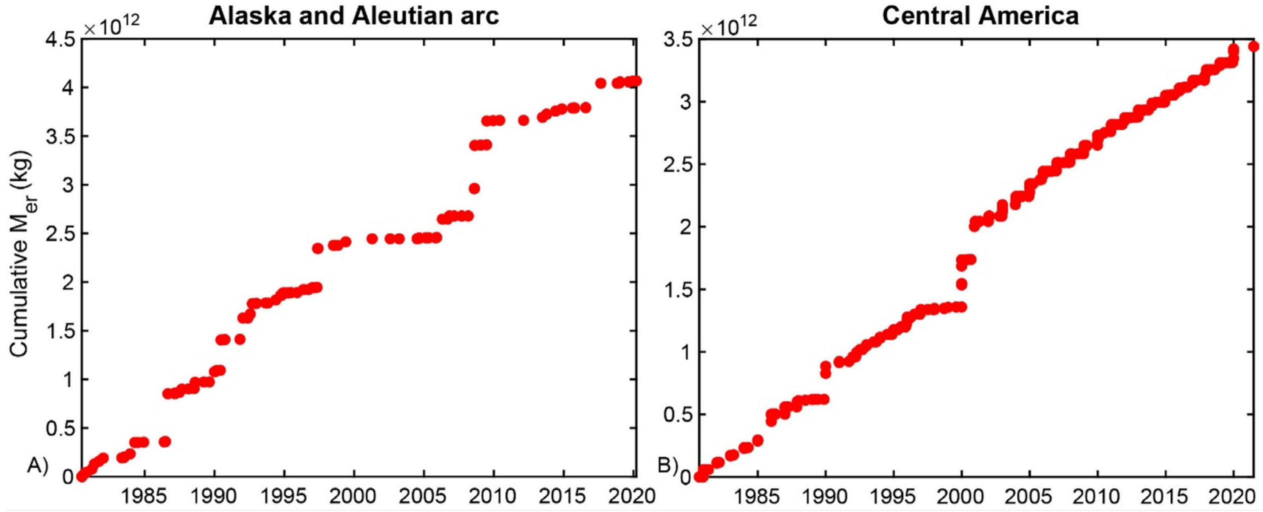

Figure 9: Cumulative masses erupted along the Alaska – Aleutian arc [A] and along the Central America arc [B] from 1980 to 2019 using data in Galetto et al. [2023a]. Central America here includes volcanoes in Guatemala, El Salvador, Honduras, Nicaragua, and Costa Rica.

Zimmerer 2022]. Thus, a future challenge would be to try building curves of cumulative erupted volumes from decadal to centuries (or longer) to investigate the possible relationship between the decadal and the centennial to millennial steady-state activity, both at the local scale of a single volcano and, although more difficult, at the regional scale of the magmatic province. At Piton de la Fournaise, the steady-state rates of the two analysed episodes are higher than the long-term rates estimated for the last 2 million years (Figure 5), while at Hawaiʻi the rates of the first and the second episode are respectively lower than and almost equal to the long-term rates estimated by White et al. [2006] for the last 0.4–0.5 million years (Figure 6D). However, the estimation of rates over a such long period is affected by many factors and might not be representative of the rates that occurred in the last millennia [Bablon et al. 2020; Galetto et al. 2023a]. For example, at Hawaiʻi the average rates of 0.07 $km^3\ yr^{-1}$ computed for the last kiloyears might be more representative of the recent volcanic activity [Lipman 1995; Quane et al. 2000], with these rates that also open to the possibility that the two observed episodes (1923–1984 and 1984–2023) might represent type IV behaviour occurring over a longer timespan (~1 century; Figure 6D). For Iceland we observe a good consistency between the eruptive rates estimated by Thordarson and Larsen [2007] for the last 1100 years and the steady-state eruptive rates from 1960 to the present (Figure 3). These rates, however, are significantly higher than the 0.02 and the 0.04 $km^3\ yr^{-1}$ estimated by White et al. [2006] for the last million years and the last 11×10^3 years, respectively. Thus, a deeper analysis of the eruptive rates over different timescales would be important to see if changes in the short-term steady sate rates can be framed within longer term steady-state periods, although these latter are more difficult to estimate. Furthermore, many long-term rates have been estimated by old data, often acquired between the 1960s and the 1970 [Crisp 1984; Gerlach 1990; White et al. 2006] and thus some updates would be necessary.

5.3 Future perspective

Due to the relationship between steady-state volcanism and volcanic hazards, it is important to identify volcanoes and magmatic provinces that are experiencing steady sate volcanism. Recently developed methods allow the improved estimation of the erupted volumes including the use of remote sensing data that allows for near global monitoring [Harris et al. 2007; Coppola et al. 2009; Ripepe et al. 2013; Kubanek et al. 2015; Bagnardi et al. 2016; Coppola et al. 2017; Dai and Howat 2017; Coppola et al. 2021; De Beni et al. 2021; Shevchenko et al. 2021; Coppola et al. 2022; Plank et al. 2023; Galetto et al. 2024; 2025].

Another important goal is to extend the analysis of the steady-state activity to other magmatic provinces. Here we focused on oceanic hotspot magmatic provinces, which provide an ideal case study since they erupt frequently with well-constrained erupted volumes. More difficult is the identification of steady-state volcanism in arcs. In Figure 9, we used data from Galetto et al. [2023a] to show some arcs (the Alaska-Aleutian and the Central America arcs) that might be exhbiting steady-state activity. However, for many arcs the analysis of possible steady-state volcanism should be performed over a timespan longer than the 40 years analyzed by Galetto et al. [2023a], due to the nature of volcanism characterizing many arcs, with quick large explosive eruptions and long quiescent times.

6 Conclusions

Here we show that Iceland, La Réunion, Hawaiʻi, and the western Galápagos volcanoes are all experiencing steady-state eruptive activity over the course of decades, despite the fact that while volcanism in Iceland and western Galápagos is distributed, at La Réunion and Hawaiʻi volcanism is localized. Understanding the steady-state regime is important, since it provides an empirical, but useful, tool to try forecasting the maximum expected erupted volumes of paroxysms or the repose time, helping the evaluation of volcanic hazards [Bonaccorso and Calvari 2013; Calvari et al. 2020; Calvari and Nunnari 2022]. For this reason, it is important to identify, study, and understand the steady-state activity in volcanoes and magmatic provinces worldwide. Our data also confirm the fact that after many decades, the steady-state regime can suddenly shift to different steady-state rates, starting a new episode. The investigation of how the steady-state rate, as well as how the changes in the steady-state rates between episodes, relate to the longer-term rates might further improve the understanding of the volcanic activity and should be pursued in future studies, despite the difficulty in constraining the eruptive rates over long timescales.

Author Contributions

F. Galetto conceptualized the project, collected the data and wrote the first draft of the manuscript. B. Asfora developed and performed the statistical analysis and wrote the associated text. M. E. Pritchard contributed to the conceptualization of the work, the writing and editing of the manuscript, provided valuable information for the discussions and interpretation of the results, and secured fundings. All Authors contributed ideas and input to the research and writing of the manuscript.

Acknowledgements

F. Galetto and M. E. Pritchard were supported by NASA Grant 80NSSC20K1674 from the Interdisciplinary Science Program of the Earth Science Division.

We are grateful to the Editor Magdalena Oryaëlle Chevrel for the helpful comments and suggestions and for the assistance in the editorial process, and to Matt Patrick and other two anonymous reviewers for their helpful comments and suggestions that improved the quality of this manuscript.

Data Availability

Codes for the Q-line fitting method and the deterministic time interval method, as well as the dataset used in Figures 7–8, have been uploaded in a public repository and are available at `https://github.com/basfora/ssvolcanism`.

Datasets reported in Figure 3–6 are reported in Galetto [2026] Tables S1–S4. All the Supplementary files (Tables S1–S6, Text S1–S4, Figures S1–S8) have been uploaded also in a permanent data repository and are available at `https://doi.org/10.17605/OSF.IO/HR4XT` [Galetto 2026]. Data in Figure 3–6 come from the following references, also reported in Supplementary Material Tables S1–S4:

Stearns and Macdonald [1946], Macdonald and Hubbard [1961], Thorarinsson and Sigvaldason [1962], Swanson [1972], Williams and Moore [1976], Macdonald et al. [1983], Dzurisin et al. [1984], Tryggvason [1984], Tryggvason [1986], Lockwood and Lipman [1987], Wolfe [1988], Chadwick et al. [1991], Guðmundsson and Björnsson [1991], Dvorak and Dzurisin [1993], Rowland [1996], Gudmundsson et al. [1997], Jónsson et al. [1999], Harris et al. [2000], Naumann and Geist [2000], Naumann [2002], Heliker and Mattox [2003], Rowland et al. [2003], Sturkell et al. [2003], Sutton et al. [2003], Teasdale et al. [2005], Geist et al. [2008], Peltier et al. [2009], Thordarson and Sigmarsson [2009], Chadwick et al. [2011], Bagnardi and Amelung [2012], Gudmundsson et al. [2012], Jude-Eton et al. [2012], Roult et al. [2012], Bagnardi et al. [2013], Hreinsdóttir et al. [2014], Wright and Klein [2014], Orr et al. [2015], Schipper et al. [2015], Gudmundsson et al. [2016], Staudacher et al. [2016], Xu et al. [2016], De Novellis et al. [2017], Pedersen et al. [2018], Peltier et al. [2018], Vasconez et al. [2018], Bernard et al. [2019], Derrien [2019], Galetto et al. [2019], Guo et al. [2019], Howard et al. [2019], Neal et al. [2019], Galetto et al. [2020], Kauahikaua and Trusdell [2020], Peltier et al. [2020], Aubry et al. [2021], Davis et al. [2021], Dietterich et al. [2021], OVPF-IPGP [2021], Blasizzo et al. [2022], Chevrel et al. [2022], Dumont et al. [2022], Pedersen et al. [2022], Chevrel et al. [2023], Galetto [2023], Galetto et al. [2023b], Parks et al. [2023], Shreve and Delgado [2023], Xu et al. [2023], Caracciolo et al. [2024], Galetto et al. [2024], Mulliken et al. [2024], Pedersen et al. [2024], Reddin et al. [2024], Campus et al. [2025], Galetto et al. [2025], Hrysiewicz et al. [2025], Parks et al. [2025], and Venzke [2025].

Copyright notice

References

Aubry, T. J., S. Engwell, C. Bonadonna, G. Carazzo, S. Scollo, A. R. Van Eaton, I. A. Taylor, D. Jessop, J. Eychenne, M. Gouhier, L. G. Mastin, K. L. Wallace, S. Biass, M. Bursik, R. G. Grainger, A. M. Jellinek, and A. Schmidt (2021). "The Independent Volcanic Eruption Source Parameter Archive (IVESPA, version 1.0): A new observational database to support explosive eruptive column model validation and development". *Journal of Volcanology and Geothermal Research* 417, page 107295. DOI: 10.1016/j.jvolgeores.2021.107295.

Bablon, M., X. Quidelleur, P. Samaniego, J.-L. Le Pennec, S. Santamaría, C. Liorzou, S. Hidalgo, and B. Eschbach (2020). "Volcanic history reconstruction in northern Ecuador: insights for eruptive and erosion rates on the whole Ecuadorian arc". *Bulletin of Volcanology* 82(1). DOI: 10.1007/s00445-019-1346-1.

Bagnardi, M. and F. Amelung (2012). "Space-geodetic evidence for multiple magma reservoirs and subvolcanic lateral intrusions at Fernandina Volcano, Galápagos Islands". *Journal of Geophysical Research: Solid Earth* 117(B10). DOI: 10.1029/2012jb009465.

Bagnardi, M., F. Amelung, and M. P. Poland (2013). "A new model for the growth of basaltic shields based on deformation of Fernandina volcano, Galápagos Islands". *Earth and Planetary Science Letters* 377–378, pages 358–366. DOI: 10.1016/j.epsl.2013.07.016.

Bagnardi, M., P. J. González, and A. Hooper (2016). "High-resolution digital elevation model from tri-stereo Pleiades-1 satellite imagery for lava flow volume estimates at Fogo

Volcano". *Geophysical Research Letters* 43(12), pages 6267–6275. DOI: 10.1002/2016gl069457.

Bebbington, M. S. (2014). "Long-term forecasting of volcanic explosivity". *Geophysical Journal International* 197(3), pages 1500–1515. DOI: 10.1093/gji/ggu078.

Bernard, B., M. J. Stock, D. Coppola, S. Hidalgo, M. Bagnardi, S. Gibson, S. Hernandez, P. Ramón, and M. Gleeson (2019). "Chronology and phenomenology of the 1982 and 2015 Wolf volcano eruptions, Galápagos Archipelago". *Journal of Volcanology and Geothermal Research* 374, pages 26–38. DOI: 10.1016/j.jvolgeores.2019.02.013.

Blasizzo, A. Y., I. A. Ukstins, S. P. Scheidt, A. H. Graettinger, D. W. Peate, T. L. Carley, A. J. Moritz, and J. E. Thines (2022). "Vikrahraun—the 1961 basaltic lava flow eruption at Askja, Iceland: morphology, geochemistry, and planetary analogs". *Earth, Planets and Space* 74(1). DOI: 10.1186/s40623-022-01711-5.

Bonaccorso, A. and S. Calvari (2013). "Major effusive eruptions and recent lava fountains: Balance between expected and erupted magma volumes at Etna volcano". *Geophysical Research Letters* 40(23), pages 6069–6073. DOI: 10.1002/2013gl058291.

Burgi, P.-Y., S. Valade, D. Coppola, G. Boudoire, G. Mavonga, F. Rufino, and D. Tedesco (2021). "Unconventional filling dynamics of a pit crater". *Earth and Planetary Science Letters* 576, page 117230. DOI: 10.1016/j.epsl.2021.117230.

Calvari, S., G. Bilotta, A. Bonaccorso, T. Caltabiano, A. Cappello, C. Corradino, C. Del Negro, G. Ganci, M. Neri, E. Pecora, G. G. Salerno, and L. Spampinato (2020). "The VEI 2 Christmas 2018 Etna Eruption: A Small But Intense Eruptive Event or the Starting Phase of a Larger One?" *Remote Sensing* 12(6), page 905. DOI: 10.3390/rs12060905.

Calvari, S. and G. Nunnari (2022). "Etna Output Rate during the Last Decade (2011–2022): Insights for Hazard Assessment". *Remote Sensing* 14(23), page 6183. DOI: 10.3390/rs14236183.

Campus, A., N. Villeneuve, O. Chevrel, A. Peltier, A. Di Muro, and D. Coppola (2025). "Effusion Rate Trends at Piton de la Fournaise: A Review of 24 Years of Space-Based Thermal Observation". *Journal of Geophysical Research: Solid Earth* 130(6). DOI: 10.1029/2024jb030962.

Cappello, A., G. Ganci, G. Bilotta, C. Corradino, A. Hérault, and C. Del Negro (2019). "Changing Eruptive Styles at the South-East Crater of Mount Etna: Implications for Assessing Lava Flow Hazards". *Frontiers in Earth Science* 7. DOI: 10.3389/feart.2019.00213.

Caracciolo, A., E. Bali, E. Ranta, S. Halldórsson, G. Guðfinnsson, and B. Óskarsson (2024). "Medieval and recent SO2 budgets in the Reykjanes Peninsula: implication for future hazard". *Geochemical Perspectives Letters* 30, pages 20–27. DOI: 10.7185/geochemlet.2417.

Chadwick, W. W., T. De Roy, and A. Carrasco (1991). "The September 1988 intracaldera avalanche and eruption at Fernandina volcano, Galapagos Islands". *Bulletin of Volcanology* 53(4), pages 276–286. DOI: 10.1007/bf00414524.

Chadwick, W. W., S. Jónsson, D. J. Geist, M. Poland, D. J. Johnson, S. Batt, K. S. Harpp, and A. Ruiz (2011). "The May 2005 eruption of Fernandina volcano, Galápagos: The first circumferential dike intrusion observed by GPS and InSAR". *Bulletin of Volcanology* 73(6), pages 679–697. DOI: 10.1007/s00445-010-0433-0.

Chevrel, M. O., A. Harris, A. Peltier, N. Villeneuve, D. Coppola, M. Gouhier, and S. Drenne (2022). "Volcanic crisis management supported by near real-time lava flow hazard assessment at Piton de la Fournaise, La Réunion". *Volcanica* 5(2), pages 313–334. DOI: 10.30909/vol.05.02.313334.

Chevrel, M. O., N. Villeneuve, R. Grandin, J.-L. Froger, D. Coppola, F. Massimetti, A. Campus, A. Hrysiewicz, and A. Peltier (2023). "Lava flow daily monitoring: the case of the 19 September–5 October 2022 eruption at Piton de la Fournaise". *Volcanica* 6(2), pages 391–404. DOI: 10.30909/vol.06.02.391404.

Civetta, L., Y. Cornette, P. Y. Gillot, and G. Orsi (1988). "The eruptive history of Pantelleria (Sicily channel) in the last 50 ka". *Bulletin of Volcanology* 50(1), pages 47–57. DOI: 10.1007/bf01047508.

Clocchiatti, R., M. Condomines, N. Guénot, and J.-C. Tanguy (2004). "Magma changes at Mount Etna: the 2001 and 2002–2003 eruptions". *Earth and Planetary Science Letters* 226(3–4), pages 397–414. DOI: 10.1016/j.epsl.2004.07.039.

Coppola, D., M. Laiolo, A. Franchi, F. Massimetti, C. Cigolini, and L. Lara (2017). "Measuring effusion rates of obsidian lava flows by means of satellite thermal data". *Journal of Volcanology and Geothermal Research* 347, pages 82–90. DOI: 10.1016/j.jvolgeores.2017.09.003.

Coppola, D., D. Piscopo, T. Staudacher, and C. Cigolini (2009). "Lava discharge rate and effusive pattern at Piton de la Fournaise from MODIS data". *Journal of Volcanology and Geothermal Research* 184(1–2), pages 174–192. DOI: 10.1016/j.jvolgeores.2008.11.031.

Coppola, D., S. Valade, P. Masias, M. Laiolo, F. Massimetti, A. Campus, R. Aguilar, R. Anccasi, F. Apaza, B. Ccallata, C. Cigolini, L. F. Cruz, A. Finizola, K. Gonzales, O. Macedo, R. Miranda, M. Ortega, R. Paxi, E. Taipe, and D. Valdivia (2022). "Shallow magma convection evidenced by excess degassing and thermal radiation during the dome-forming Sabancaya eruption (2012–2020)". *Bulletin of Volcanology* 84(2). DOI: 10.1007/s00445-022-01523-1.

Coppola, D., M. Laiolo, F. Massimetti, S. Hainzl, A. V. Shevchenko, R. Mania, N. M. Shapiro, and T. R. Walter (2021). "Thermal remote sensing reveals communication between volcanoes of the Klyuchevskoy Volcanic Group". *Scientific Reports* 11(1). DOI: 10.1038/s41598-021-92542-z.

Crisp, J. A. (1984). "Rates of magma emplacement and volcanic output". *Journal of Volcanology and Geothermal Research* 20(3–4), pages 177–211. DOI: 10.1016/0377-0273(84)90039-8.

Dai, C. and I. M. Howat (2017). "Measuring Lava Flows With ArcticDEM: Application to the 2012–2013 Eruption of Tolbachik, Kamchatka". *Geophysical Research Letters* 44(24). DOI: 10.1002/2017gl075920.

Davis, T., M. Bagnardi, P. Lundgren, and E. Rivalta (2021). "Extreme Curvature of Shallow Magma Pathways Controlled by Competing Stresses: Insights From the 2018 Sierra Negra Eruption". Geophysical Research Letters 48(13). DOI: 10.1029/2021gl093038.

De Beni, E., M. Cantarero, M. Neri, and A. Messina (2021). "Lava flows of Mt Etna, Italy: the 2019 eruption within the context of the last two decades (1999–2019)". Journal of Maps 17(3), pages 65–76. DOI: 10.1080/17445647.2020.1854131.

De la Cruz-Reyna, S. (1991). "Poisson-distributed patterns of explosive eruptive activity". Bulletin of Volcanology 54(1), pages 57–67. DOI: 10.1007/bf00278206.

De Novellis, V., R. Castaldo, C. De Luca, S. Pepe, I. Zinno, F. Casu, R. Lanari, and G. Solaro (2017). "Source modelling of the 2015 Wolf volcano (Galápagos) eruption inferred from Sentinel 1-A DInSAR deformation maps and pre-eruptive ENVISAT time series". Journal of Volcanology and Geothermal Research 344, pages 246–256. DOI: 10.1016/j.jvolgeores.2017.05.013.

Derrien, A. (2019). "Apports des techniques photogrammétriques à l'étude du dynamisme des structures volcaniques du piton de la Fournaise". PhD thesis. Université Paris Cité.

Di Renzo, V., R. Corsaro, L. Miraglia, M. Pompilio, and L. Civetta (2019). "Long and short-term magma differentiation at Mt. Etna as revealed by Sr-Nd isotopes and geochemical data". Earth-Science Reviews 190, pages 112–130. DOI: 10.1016/j.earscirev.2018.12.008.

Dietterich, H. R., A. K. Diefenbach, S. A. Soule, M. H. Zoeller, M. P. Patrick, J. J. Major, and P. R. Lundgren (2021). "Lava effusion rate evolution and erupted volume during the 2018 Kīlauea lower East Rift Zone eruption". Bulletin of Volcanology 83(4). DOI: 10.1007/s00445-021-01443-6.

Dumont, Q., V. Cayol, J.-L. Froger, and A. Peltier (2022). "22 years of satellite imagery reveal a major destabilization structure at Piton de la Fournaise". Nature Communications 13(1). DOI: 10.1038/s41467-022-30109-w.

Dvorak, J. J. and D. Dzurisin (1993). "Variations in magma supply rate at Kilauea Volcano, Hawaii". Journal of Geophysical Research: Solid Earth 98(B12), pages 22255–22268. DOI: 10.1029/93jb02765.

Dzurisin, D., R. Y. Koyanagi, and T. T. English (1984). "Magma supply and storage at Kilauea volcano, Hawaii, 1956–1983". Journal of Volcanology and Geothermal Research 21(3–4), pages 177–206. DOI: 10.1016/0377-0273(84)90022-2.

Galetto, F. (2023). "Complex paths of magma propagation at Fernandina (Galápagos): The coexistence of circumferential and radial dike intrusion during the January 2020 eruption". Bulletin of Volcanology 85(12). DOI: 10.1007/s00445-023-01688-3.

– (2026). "Supplementary Material to: "Evaluating steady-state volcanism in Iceland, La Réunion, Hawai'i and western Galápagos: connections with volcanic hazards and future perspectives"". Open Science Framework. DOI: 10.17605/OSF.IO/HR4XT. [Dataset].

Galetto, F., M. Bagnardi, V. Acocella, and A. Hooper (2019). "Noneruptive Unrest at the Caldera of Alcedo Volcano (Galápagos Islands) Revealed by InSAR Data and Geodetic Modeling". Journal of Geophysical Research: Solid Earth 124(4), pages 3365–3381. DOI: 10.1029/2018jb017103.

Galetto, F., E. Dualeh, F. Delgado, M. Pritchard, M. Poland, S. Ebmeier, T. Shreve, J. Biggs, I. Hamling, C. Wauthier, J. Gonzalez Santana, J.-L. Froger, and M. Bemelmans (2024). "The utility of TerraSAR-X, TanDEM-X, and PAZ for studying global volcanic activity: Successes, challenges, and future prospects". Volcanica 7(1), pages 273–301. DOI: 10.30909/vol.07.01.273301.

Galetto, F., A. Hooper, M. Bagnardi, and V. Acocella (2020). "The 2008 Eruptive Unrest at Cerro Azul Volcano (Galápagos) Revealed by InSAR Data and a Novel Method for Geodetic Modelling". Journal of Geophysical Research: Solid Earth 125(2). DOI: 10.1029/2019jb018521.

Galetto, F., S. M. Miller, R. Barris, A. V. Shevchenko, and M. E. Pritchard (2025). "The application of high resolution EarthDEM and ArcticDEM digital elevation models to detect and quantify volcanic activity: successes and challenges". Bulletin of Volcanology 87(7). DOI: 10.1007/s00445-025-01838-9.

Galetto, F., M. E. Pritchard, A. J. Hornby, E. Gazel, and N. M. Mahowald (2023a). "Spatial and Temporal Quantification of Subaerial Volcanism From 1980 to 2019: Solid Products, Masses, and Average Eruptive Rates". Reviews of Geophysics 61(1). DOI: 10.1029/2022rg000783.

Galetto, F., D. Reale, E. Sansosti, and V. Acocella (2023b). "Implications for Shallow Magma Transfer During the 2017 and 2018 Eruptions at Fernandina (Galápagos) Inferred From InSAR Data". Journal of Geophysical Research: Solid Earth 128(6). DOI: 10.1029/2022jb026174.

Geist, D., K. A. Howard, A. M. Jellinek, and S. Rayder (1994). "The volcanic history of Volcán Alcedo, Galápagos Archipelago: A case study of rhyolitic oceanic volcanism". Bulletin of Volcanology 56(4), pages 243–260. DOI: 10.1007/bf00302078.

Geist, D. J. (1996). "On the emergence and submergence of the Galápagos Islands". Noticias de Galápagos 56, pages 5–9.

Geist, D. J., G. Bergantz, and W. W. Chadwick (2014). Galápagos Magma Chambers. DOI: 10.1002/9781118852538.ch5.

Geist, D. J., K. S. Harpp, T. R. Naumann, M. Poland, W. W. Chadwick, M. Hall, and E. Rader (2008). "The 2005 eruption of Sierra Negra volcano, Galápagos, Ecuador". Bulletin of Volcanology 70(6), pages 655–673. DOI: 10.1007/s00445-007-0160-3.

Geist, D. J., T. R. Naumann, J. J. Standish, M. D. Kurz, K. S. Harpp, W. M. Whte, and D. J. Fornari (2005). "Wolf Volcano, Galápagos Archipelago: Melting and Magmatic Evolution at the Margins of a Mantle Plume". Journal of Petrology 46(11), pages 2197–2224. DOI: 10.1093/petrology/egi052.

Gerlach, D. C. (1990). "Eruption rates and isotopic systematics of ocean islands: further evidence for small-scale heterogeneity in the upper mantle". Tectonophysics 172(3–4), pages 273–289. DOI: 10.1016/0040-1951(90)90035-7.

Greene, A. R., M. O. Garcia, A. J. Pietruszka, D. Weis, J. P. Marske, M. J. Vollinger, and J. Eiler (2013). "Temporal geochemical variations in lavas from Kīlauea's Pu'u 'Ō'ō eruption (1983–2010): Cyclic variations from melting of source heterogeneities". *Geochemistry, Geophysics, Geosystems* 14(11), pages 4849–4873. DOI: 10.1002/ggge.20285.

Gudmundsson, M. T., F. Sigmundsson, and H. Björnsson (1997). "Ice–volcano interaction of the 1996 Gjálp subglacial eruption, Vatnajökull, Iceland". *Nature* 389(6654), pages 954–957. DOI: 10.1038/40122.

Gudmundsson, M. T., K. Jónsdóttir, A. Hooper, E. P. Holohan, S. A. Halldórsson, B. G. Ófeigsson, S. Cesca, K. S. Vogfjörd, F. Sigmundsson, T. Högnadóttir, P. Einarsson, O. Sigmarsson, A. H. Jarosch, K. Jónasson, E. Magnússon, S. Hreinsdóttir, M. Bagnardi, M. M. Parks, V. Hjörleifsdóttir, F. Pálsson, T. R. Walter, M. P. J. Schöpfer, S. Heimann, H. I. Reynolds, S. Dumont, E. Bali, G. H. Gudfinnsson, T. Dahm, M. J. Roberts, M. Hensch, J. M. C. Belart, K. Spaans, S. Jakobsson, G. B. Gudmundsson, H. M. Fridriksdóttir, V. Drouin, T. Dürig, G. Aðalgeirsdóttir, M. S. Riishuus, G. B. M. Pedersen, T. van Boeckel, B. Oddsson, M. A. Pfeffer, S. Barsotti, B. Bergsson, A. Donovan, M. R. Burton, and A. Aiuppa (2016). "Gradual caldera collapse at Bárdarbunga volcano, Iceland, regulated by lateral magma outflow". *Science* 353(6296). DOI: 10.1126/science.aaf8988.

Gudmundsson, M. T., T. Thordarson, Á. Höskuldsson, G. Larsen, H. Björnsson, F. J. Prata, B. Oddsson, E. Magnússon, T. Högnadóttir, G. N. Petersen, C. L. Hayward, J. A. Stevenson, and I. Jónsdóttir (2012). "Ash generation and distribution from the April-May 2010 eruption of Eyjafjallajökull, Iceland". *Scientific Reports* 2(1). DOI: 10.1038/srep00572.

Guðmundsson, M. T. and H. Björnsson (1991). "Eruptions in Grímsvötn, Vatnajökull, Iceland, 1934–1991". *Jökull* 41(1), pages 21–45. DOI: 10.33799/jokull1991.41.021.

Guo, Q., C. Xu, Y. Wen, Y. Liu, and G. Xu (2019). "The 2017 Noneruptive Unrest at the Caldera of Cerro Azul Volcano (Galápagos Islands) Revealed by InSAR Observations and Geodetic Modelling". *Remote Sensing* 11(17), page 1992. DOI: 10.3390/rs11171992.

Harpp, K. S. and D. J. Geist (2018). "The Evolution of Galápagos Volcanoes: An Alternative Perspective". *Frontiers in Earth Science* 6. DOI: 10.3389/feart.2018.00050.

Harris, A., J. Murray, S. Aries, M. Davies, L. Flynn, M. Wooster, R. Wright, and D. Rothery (2000). "Effusion rate trends at Etna and Krafla and their implications for eruptive mechanisms". *Journal of Volcanology and Geothermal Research* 102(3–4), pages 237–269. DOI: 10.1016/s0377-0273(00)00190-6.

Harris, A., A. Steffke, S. Calvari, and L. Spampinato (2011). "Thirty years of satellite-derived lava discharge rates at Etna: Implications for steady volumetric output". *Journal of Geophysical Research* 116(B8). DOI: 10.1029/2011jb008237.

Harris, A. J. L., J. Dehn, and S. Calvari (2007). "Lava effusion rate definition and measurement: a review". *Bulletin of Volcanology* 70(1), pages 1–22. DOI: 10.1007/s00445-007-0120-y.

Heliker, C. and T. N. Mattox (2003). "The First Two Decades of the Puʻu ʻŌʻō–Kūpaianaha Eruption: Chronology and Selected Bibliography". *The Puʻu ʻŌʻō–Kūpaianaha Eruption of Kīlauea Volcano, Hawaiʻi: The First 20 Years*. Edited by C. C. Heliker, D. A. Swanson, and T. J. Takahashi. U.S. Geological Survey Professional Paper 1676. Reston, VA: U.S. Geological Survey. DOI: 10.3133/pp1676.

Howard, K. A., T. Simkin, D. J. Geist, G. Merlen, and B. Nolf (2019). "Large hydromagmatic eruption related to Fernandina Volcano's 1968 caldera collapse—Deposits, landforms, and ecosystem recovery". *Field Volcanology: A Tribute to the Distinguished Career of Don Swanson*. Edited by M. P. Poland, M. O. Garcia, V. E. Camp, and A. Grunder. Geological Society of America, pages 385–408. ISBN: 9780813795386. DOI: 10.1130/2018.2538(18).

Hreinsdóttir, S., F. Sigmundsson, M. J. Roberts, H. Björnsson, R. Grapenthin, P. Arason, T. Árnadóttir, J. Hólmjárn, H. Geirsson, R. A. Bennett, M. T. Gudmundsson, B. Oddsson, B. G. Ófeigsson, T. Villemin, T. Jónsson, E. Sturkell, Á. Höskuldsson, G. Larsen, T. Thordarson, and B. A. Óladóttir (2014). "Volcanic plume height correlated with magma-pressure change at Grímsvötn Volcano, Iceland". *Nature Geoscience* 7(3), pages 214–218. DOI: 10.1038/ngeo2044.

Hrysiewicz, A., P. C. LaFemina, A. Bell, F. Galetto, S. Vallejo, B. Bernard, and E. P. Holohan (2025). "Lava Tube System Development Defined by Multispectral Imaging and InSAR: The Case of the 2024 Eruption of Fernandina Volcano (Galápagos)". *Journal of Geophysical Research: Solid Earth* 130(11). DOI: 10.1029/2025jb032265.

Jicha, B. R. and B. S. Singer (2006). "Volcanic history and magmatic evolution of Seguam Island, Aleutian Island arc, Alaska". *Geological Society of America Bulletin* 118(7–8), pages 805–822. DOI: 10.1130/b25861.1.

Jónsson, S., H. Zebker, P. Cervelli, P. Segall, H. Garbeil, P. Mouginis-Mark, and S. Rowland (1999). "A shallow-dipping dike fed the 1995 flank eruption at Fernandina Volcano, Galápagos, observed by satellite radar interferometry". *Geophysical Research Letters* 26(8), pages 1077–1080. DOI: 10.1029/1999gl900108.

Jude-Eton, T. C., T. Thordarson, M. T. Gudmundsson, and B. Oddsson (2012). "Dynamics, stratigraphy and proximal dispersal of supraglacial tephra during the ice-confined 2004 eruption at Grímsvötn Volcano, Iceland". *Bulletin of Volcanology* 74(5), pages 1057–1082. DOI: 10.1007/s00445-012-0583-3.

Kauahikaua, J. P. and F. A. Trusdell (2020). *Have humans influenced volcanic activity on the lower East Rift Zone of Kīlauea Volcano? A publication review*. DOI: 10.3133/ofr20201017.

King, C.-Y. (1989). "Volume predictability of historical eruptions at Kilauea and Mauna Loa volcanoes". *Journal of Volcanology and Geothermal Research* 38(3–4), pages 281–285. DOI: 10.1016/0377-0273(89)90043-7.

Klein, F. W., R. Y. Koyanagi, J. S. Nakata, and W. R. Tanigawa (1987). "The Seismicity of Kilauea's Magma System". *Volcanism in Hawaii*. Edited by R. W. Decker, T. L. Wright, and P. H. Stauffer. U.S. Geological Survey Professional Paper 1350. U.S. Geological Survey. Chapter 43, pages 1019–1185. DOI: 10.3133/pp1350.

Kubanek, J., M. Westerhaus, A. Schenk, N. Aisyah, K. S. Brotopuspito, and B. Heck (2015). "Volumetric change quantification of the 2010 Merapi eruption using TanDEM-X InSAR".

Remote Sensing of Environment 164, pages 16–25. DOI: 10.1016/j.rse.2015.02.027.

Kuntz, M. A., D. E. Champion, E. C. Spiker, and R. H. Lefebvre (1986). "Contrasting magma types and steady-state, volume-predictable, basaltic volcanism along the Great Rift, Idaho". *Geological Society of America Bulletin* 97(5), page 579. DOI: 10.1130/0016-7606(1986)97<579:cmtasv>2.0.co;2.

Kurz, M. D., S. K. Rowland, J. Curtice, A. E. Saal, and T. Naumann (2014). *Eruption Rates for Fernandina Volcano: A New Chronology at the Galápagos Hotspot Center*. DOI: 10.1002/9781118852538.ch4.

Lipman, P. W. (1995). "Declining Growth of Mauna Loa During the Last 100,000 Years: Rates of Lava Accumulation vs. Gravitational Subsidence". *Mauna Loa Revealed: Structure, Composition, History, and Hazards*. Volume 92. Geophysical Monograph, pages 45–80. DOI: 10.1029/GM092p0045.

– (2000). "Central San Juan caldera cluster: regional volcanic framework". *Special Paper 346: Ancient Lake Creede: its volcano-tectonic setting, history of sedimentation, and relation to mineralization in the Creede mining district*. Geological Society of America, pages 9–69. ISBN: 0813723469. DOI: 10.1130/0-8137-2346-9.9.

Lockwood, J. P. and P. W. Lipman (1987). "Holocene Eruptive History of Mauna Loa Volcano". *Volcanism in Hawaii*. Edited by R. W. Decker, T. L. Wright, and P. H. Stauffer. U.S. Geological Survey Professional Paper 1350. U.S. Geological Survey. Chapter 18, pages 509–535. DOI: 10.3133/pp1350.

Macdonald, G. A., A. T. Abbott, and F. L. Peterson (1983). *Volcanoes in the Sea: The Geology of Hawaii*. 2nd edition. Honolulu: University of Hawaii Press. 544 pages. ISBN: 978-0824808327.

Macdonald, G. A. and D. H. Hubbard (1961). *Volcanoes of the National Parks in Hawaii*. Honolulu: Hawaii Natural History Association. 64 pages. ISBN: 978-0940295018.

Marturano, A., R. Isaia, G. Aiello, and D. Barra (2018). "Complex Dome Growth at Campi Flegrei Caldera (Italy) in the Last 15 ka". *Journal of Geophysical Research: Solid Earth* 123(9), pages 8180–8197. DOI: 10.1029/2018jb015672.

Montgomery-Brown, E. K. and A. Miklius (2020). "Periodic dike intrusions at Kīlauea volcano, Hawai'i". *Geology* 49(4), pages 397–401. DOI: 10.1130/g47970.1.

Moore, J. G. (1970). "Relationship Between Subsidence and Volcanic Load, Hawaii". *Bulletin Volcanologique* 34(2), pages 562–576.

Mulliken, K. M., J. P. Kauahikaua, D. A. Swanson, and M. H. Zoeller (2024). *Chronology of Recent Volcanic Activity on the Island of Hawai'i, Hawaii*. Data Release 76. U.S. Geological Survey.

Nasholds, M. W. and M. J. Zimmerer (2022). "High-precision 40Ar/39Ar geochronology and volumetric investigation of volcanism and resurgence following eruption of the Tshirege Member, Bandelier Tuff, at the Valles caldera". *Journal of Volcanology and Geothermal Research* 431, page 107624. DOI: 10.1016/j.jvolgeores.2022.107624.

Naumann, T. (2002). "Petrology and Geochemistry of Volcan Cerro Azul: Petrologic Diversity among the Western Galapagos Volcanoes". *Journal of Petrology* 43(5), pages 859–883. DOI: 10.1093/petrology/43.5.859.

Naumann, T. and D. Geist (2000). "Physical volcanology and structural development of Cerro Azul Volcano, Isabela Island, Galápagos: implications for the development of Galápagos-type shield volcanoes". *Bulletin of Volcanology* 61(8), pages 497–514. DOI: 10.1007/s004450050001.

Neal, C. A., S. R. Brantley, L. Antolik, J. L. Babb, M. Burgess, K. Calles, M. Cappos, J. C. Chang, S. Conway, L. Desmither, P. Dotray, T. Elias, P. Fukunaga, S. Fuke, I. A. Johanson, K. Kamibayashi, J. Kauahikaua, R. L. Lee, S. Pekalib, A. Miklius, W. Million, C. J. Moniz, P. A. Nadeau, P. Okubo, C. Parcheta, M. R. Patrick, B. Shiro, D. A. Swanson, W. Tollett, F. Trusdell, E. F. Younger, M. H. Zoeller, E. K. Montgomery-Brown, K. R. Anderson, M. P. Poland, J. L. Ball, J. Bard, M. Coombs, H. R. Dietterich, C. Kern, W. A. Thelen, P. F. Cervelli, T. Orr, B. F. Houghton, C. Gansecki, R. Hazlett, P. Lundgren, A. K. Diefenbach, A. H. Lerner, G. Waite, P. Kelly, L. Clor, C. Werner, K. Mulliken, G. Fisher, and D. Damby (2019). "The 2018 rift eruption and summit collapse of Kīlauea Volcano". *Science* 363(6425), pages 367–374. DOI: 10.1126/science.aav7046.

O'Hagan, A. and T. Leonard (1976). "Bayes estimation subject to uncertainty about parameter constraints". *Biometrika* 63(1), pages 201–203. DOI: 10.1093/biomet/63.1.201.

Observatoire Volcanologique du Piton de la Fournaise – Institut de Physique du Globe de Paris (OVPF-IPGP) (2021). *Rapport Annuel 2021*.

Orr, T. R., M. P. Poland, M. R. Patrick, W. A. Thelen, A. J. Sutton, T. Elias, C. R. Thornber, C. Parcheta, and K. M. Wooten (2015). *Kīlauea's 5–9 March 2011 Kamoamoa Fissure Eruption and Its Relation to 30+ Years of Activity From Pu'u 'Ō 'ō*. DOI: 10.1002/9781118872079.ch18.

Parks, M., V. Drouin, F. Sigmundsson, Á. R. Hjartardóttir, H. Geirsson, G. B. Pedersen, J. M. Belart, S. Barsotti, C. Lanzi, K. Vogfjörd, A. Hooper, B. Ófeigsson, S. Hreinsdóttir, E. B. Gestsson, R. H. Þrastarson, P. Einarsson, V. Tolpekin, D. Rotheram-Clarke, S. R. Gunnarsson, B. V. Óskarsson, and V. Pinel (2025). "2023–2024 inflation-deflation cycles at Svartsengi and repeated dike injections and eruptions at the Sundhnúkur crater row, Reykjanes Peninsula, Iceland". *Earth and Planetary Science Letters* 658, page 119324. DOI: 10.1016/j.epsl.2025.119324.

Parks, M., F. Sigmundsson, V. Drouin, Á. R. Hjartardóttir, H. Geirsson, A. Hooper, K. S. Vogfjörd, B. G. Ófeigsson, S. Hreinsdóttir, E. H. Jensen, P. Einarsson, S. Barsotti, and H. M. Fridriksdóttir (2023). "Deformation, seismicity, and monitoring response preceding and during the 2022 Fagradalsfjall eruption, Iceland". *Bulletin of Volcanology* 85(10). DOI: 10.1007/s00445-023-01671-y.

Pedersen, G. B. M., J. M. C. Belart, E. Magnússon, O. K. Vilmundardóttir, F. Kizel, F. S. Sigurmundsson, G. Gísladóttir, and J. A. Benediktsson (2018). "Hekla Volcano, Iceland, in the 20th Century: Lava Volumes, Production Rates, and Effusion Rates". *Geophysical Research Letters* 45(4), pages 1805–1813. DOI: 10.1002/2017gl076887.

Pedersen, G. B. M., J. M. C. Belart, B. V. Óskarsson, S. R. Gunnarson, M. T. Gudmundsson, H. I. Reynolds, G. Valsson, T.

Högnadóttir, V. Pinel, M. M. Parks, V. Drouin, R. A. Askew, T. Dürig, and R. H. Þrastarson (2024). "Volume, effusion rates and lava hazards of the 2021, 2022 and 2023 Reykjanes fires: Lessons learned from near real-time photogrammetric monitoring". *EGU General Assembly Abstracts*. Vienna: Copernicus GmbH. DOI: 10.5194/egusphere-egu24-10724.

Pedersen, G. B. M., J. M. C. Belart, B. V. Óskarsson, M. T. Gudmundsson, N. Gies, T. Högnadóttir, Á. R. Hjartardóttir, V. Pinel, E. Berthier, T. Dürig, H. I. Reynolds, C. W. Hamilton, G. Valsson, P. Einarsson, D. Ben-Yehosua, A. Gunnarsson, and B. Oddsson (2022). "Volume, Effusion Rate, and Lava Transport During the 2021 Fagradalsfjall Eruption: Results From Near Real-Time Photogrammetric Monitoring". *Geophysical Research Letters* 49(13). DOI: 10.1029/2021gl097125.

Peltier, A., P. Bachèlery, and T. Staudacher (2009). "Magma transport and storage at Piton de La Fournaise (La Réunion) between 1972 and 2007: A review of geophysical and geochemical data". *Journal of Volcanology and Geothermal Research* 184(1–2), pages 93–108. DOI: 10.1016/j.jvolgeores.2008.12.008.

Peltier, A., V. Ferrazzini, A. Di Muro, P. Kowalski, N. Villeneuve, N. Richter, O. Chevrel, J. L. Froger, A. Hrysiewicz, M. Gouhier, D. Coppola, L. Retailleau, F. Beauducel, L. Gurioli, P. Boissier, C. Brunet, P. Catherine, F. Fontaine, F. Lauret, L. Garavaglia, J. Lebreton, K. Canjamale, N. Desfete, C. Griot, A. Harris, S. Arellano, M. Liuzzo, S. Gurrieri, and M. Ramsey (2020). "Volcano Crisis Management at Piton de la Fournaise (La Réunion) during the COVID-19 Lockdown". *Seismological Research Letters* 92(1), pages 38–52. DOI: 10.1785/0220200212.

Peltier, A., N. Villeneuve, V. Ferrazzini, S. Testud, T. Hassen Ali, P. Boissier, and P. Catherine (2018). "Changes in the Long-Term Geophysical Eruptive Precursors at Piton de la Fournaise: Implications for the Response Management". *Frontiers in Earth Science* 6. DOI: 10.3389/feart.2018.00104.

Plank, S., A. V. Shevchenko, P. d'Angelo, V. Gstaiger, P. J. González, S. Cesca, S. Martinis, and T. R. Walter (2023). "Combining thermal, tri-stereo optical and bi-static InSAR satellite imagery for lava volume estimates: the 2021 Cumbre Vieja eruption, La Palma". *Scientific Reports* 13(1). DOI: 10.1038/s41598-023-29061-6.

Poland, M. P., A. Miklius, A. Jeff Sutton, and C. R. Thornber (2012). "A mantle-driven surge in magma supply to Kīlauea Volcano during 2003–2007". *Nature Geoscience* 5(4), pages 295–300. DOI: 10.1038/ngeo1426.

Poland, M. P., A. Miklius, and E. K. Montgomery-Brown (2014). "Magma supply, storage, and transport at shield-stage". *Characteristics of Hawaiian volcanoes*. Edited by M. P. Poland, T. J. Takahashi, and C. M. Landowski. Government Printing Office, pages 179–234. U.S. Geological Survey Professional Paper 1801.

Pouclet, A. and K. Bram (2021). "Nyiragongo and Nyamuragira: a review of volcanic activity in the Kivu rift, western branch of the East African Rift System". *Bulletin of Volcanology* 83(2). DOI: 10.1007/s00445-021-01435-6.

Quane, S., M. Garcia, H. Guillou, and T. Hulsebosch (2000). "Magmatic history of the East Rift Zone of Kilauea Volcano, Hawaii based on drill core from SOH 1". *Journal of Volcanology and Geothermal Research* 102(3–4), pages 319–338. DOI: 10.1016/s0377-0273(00)00194-3.

Reddin, E., S. Ebmeier, M. Bagnardi, A. F. Bell, and P. Espín Bedón (2024). "Craters of habit: Patterns of deformation in the western Galápagos". *Volcanica* 7(1), pages 181–227. DOI: 10.30909/vol.07.01.181227.

Reynolds, R. W., D. Geist, and M. D. Kurz (1995). "Physical volcanology and structural development of Sierra Negra volcano, Isabela Island, Gal´apagos archipelago". *Geological Society of America Bulletin* 107(12), pages 1398–1410. DOI: 10.1130/0016-7606(1995)107<1398:pvasdo>2.3.co;2.

Ripepe, M., C. Bonadonna, A. Folch, D. Delle Donne, G. Lacanna, E. Marchetti, and A. Höskuldsson (2013). "Ash-plume dynamics and eruption source parameters by infrasound and thermal imagery: The 2010 Eyjafjallajökull eruption". *Earth and Planetary Science Letters* 366, pages 112–121. DOI: 10.1016/j.epsl.2013.02.005.

Roult, G., A. Peltier, B. Taisne, T. Staudacher, V. Ferrazzini, and A. Di Muro (2012). "A new comprehensive classification of the Piton de la Fournaise activity spanning the 1985–2010 period. Search and analysis of short-term precursors from a broad-band seismological station". *Journal of Volcanology and Geothermal Research* 241–242, pages 78–104. DOI: 10.1016/j.jvolgeores.2012.06.012.

Rowland, S. K. (1996). "Slopes, lava flow volumes, and vent distributions on Volcán Fernandina, Galápagos Islands". *Journal of Geophysical Research: Solid Earth* 101(B12), pages 27657–27672. DOI: 10.1029/96jb02649.

Rowland, S. K., A. J. L. Harris, M. J. Wooster, F. Amelung, H. Garbeil, L. Wilson, and P. J. Mouginis-Mark (2003). "Volumetric characteristics of lava flows from interferometric radar and multispectral satellite data: the 1995 Fernandina and 1998 Cerro Azul eruptions in the western Galápagos". *Bulletin of Volcanology* 65(5), pages 311–330. DOI: 10.1007/s00445-002-0262-x.

Schipper, C. I., S. P. Jakobsson, J. D. White, J. M. Palin, and T. Bush-Marcinowski (2015). "The Surtsey Magma Series". *Scientific Reports* 5(1). DOI: 10.1038/srep11498.

Shevchenko, A. V., V. N. Dvigalo, E. U. Zorn, M. S. Vassileva, F. Massimetti, T. R. Walter, I. Y. Svirid, S. A. Chirkov, A. Y. Ozerov, V. A. Tsvetkov, and I. A. Borisov (2021). "Constructive and Destructive Processes During the 2018–2019 Eruption Episode at Shiveluch Volcano, Kamchatka, Studied From Satellite and Aerial Data". *Frontiers in Earth Science* 9. DOI: 10.3389/feart.2021.680051.

Shreve, T. and F. Delgado (2023). "Trapdoor Fault Activation: A Step Toward Caldera Collapse at Sierra Negra, Galápagos, Ecuador". *Journal of Geophysical Research: Solid Earth* 128(5). DOI: 10.1029/2023jb026437.

Singer, B. S., B. R. Jicha, M. A. Harper, J. A. Naranjo, L. E. Lara, and H. Moreno-Roa (2008). "Eruptive history, geochronology, and magmatic evolution of the Puyehue-Cordon Caulle volcanic complex, Chile". *Geological Society of America Bulletin* 120(5–6), pages 599–618. DOI: 10.1130/b26276.1.

Singer, B. S., R. A. Thompson, M. A. Dungan, T. C. Feeley, S. T. Nelson, J. C. Pickens, L. L. Brown, A. W. Wulff, J. P. Davidson, and J. Metzger (1997). "Volcanism and erosion during the past 930 k.y. at the Tatara–San Pedro complex, Chilean Andes". *Geological Society of America Bulletin* 109(2), pages 127–142. DOI: 10.1130/0016-7606(1997)109<0127:vaedtp>2.3.co;2.

Staudacher, T., A. Peltier, V. Ferrazzini, A. Di Muro, P. Boissier, P. Catherine, P. Kowalski, F. Lauret, and J. Lebreton (2016). "Fifteen Years of Intense Eruptive Activity (1998–2013) at Piton de la Fournaise Volcano: A Review". *Active Volcanoes of the Southwest Indian Ocean*. Springer Berlin Heidelberg, pages 139–170. ISBN: 9783642313950. DOI: 10.1007/978-3-642-31395-0_9.

Stearns, H. T. and G. A. Macdonald (1946). *Geology and Ground-Water Resources of the Island of Hawaii*. U.S. Geological Survey Bulletin 9. Hawaii Division of Hydrography. 363 pages.

Sturkell, E., P. Einarsson, F. Sigmundsson, S. Hreinsdóttir, and H. Geirsson (2003). "Deformation of Grímsvötn volcano, Iceland: 1998 eruption and subsequent inflation". *Geophysical Research Letters* 30(4). DOI: 10.1029/2002gl016460.

Sutton, A. J., T. Elias, and J. Kauahikaua (2003). "Lava-Effusion Rates for the Puʻu ʻŌʻō–Kūpaianaha Eruption Derived from SO2 Emissions and Very Low Frequency Measurements". *The Puʻu ʻŌʻō–Kūpaianaha Eruption of Kīlauea Volcano, Hawaiʻi: The First 20 Years*. Edited by C. C. Heliker, D. A. Swanson, and T. J. Takahashi. Volume 1676. U.S. Geological Survey Professional Paper. U.S. Geological Survey. DOI: 10.3133/pp1676.

Swanson, D. A. (1972). "Magma Supply Rate at Kilauea Volcano, 1952-1971". *Science* 175(4018), pages 169–170. DOI: 10.1126/science.175.4018.169.

Teasdale, R., D. Geist, M. Kurz, and K. Harpp (2005). "1998 Eruption at Volcán Cerro Azul, Galápagos Islands: I. Syn-Eruptive Petrogenesis". *Bulletin of Volcanology* 67(2), pages 170–185. DOI: 10.1007/s00445-004-0371-9.

Thorarinsson, S. and G. E. Sigvaldason (1962). "The eruption in Askja, 1961; a preliminary report". *American Journal of Science* 260(9), pages 641–651. DOI: 10.2475/ajs.260.9.641.

Thordarson, T. and G. Larsen (2007). "Volcanism in Iceland in historical time: Volcano types, eruption styles and eruptive history". *Journal of Geodynamics* 43(1), pages 118–152. DOI: 10.1016/j.jog.2006.09.005.

Thordarson, T. and O. Sigmarsson (2009). "Effusive activity in the 1963-1967 Surtsey eruption, Iceland: flow emplacement and growth of small lava shields". *Studies in Volcanology: The Legacy of George Walker*. Edited by T. Thordarson, S. Self, G. Larsen, S. K. Rowland, and Á. Höskuldsson. The Geological Society of London on behalf of The International Association of Volcanology and Chemistry of the Earth's Interior, pages 53–84. ISBN: 9781862392809. DOI: 10.1144/iavcel002.4.

Tryggvason, E. (1984). "Widening of the Krafla fissure swarm during the 1975–1981 volcano-tectonic episode". *Bulletin Volcanologique* 47(1), pages 47–69. DOI: 10.1007/bf01960540.

Tryggvason, E. (1986). "Multiple magma reservoirs in a rift zone volcano: Ground deformation and magma transport during the September 1984 eruption of Krafla, Iceland". *Journal of Volcanology and Geothermal Research* 28(1–2), pages 1–44. DOI: 10.1016/0377-0273(86)90003-x.

Vasconez, F. J., P. Ramón, S. Hernandez, S. Hidalgo, B. Bernard, M. Ruiz, A. Alvarado, P. La Femina, and G. Ruiz (2018). "The different characteristics of the recent eruptions of Fernandina and Sierra Negra volcanoes (Galápagos, Ecuador)". *Volcanica* 1(2), pages 127–133. DOI: 10.30909/vol.01.02.127133.

"Volcanoes of the World, v.5.3.1" (2025). Edited by E. Venzke. DOI: 10.5479/si.gvp.votw5-2025.5.3. [Dataset].

Viccaro, M., E. Nicotra, I. L. Millar, and R. Cristofolini (2011). "The magma source at Mount Etna volcano: Perspectives from the Hf isotope composition of historic and recent lavas". *Chemical Geology* 281(3–4), pages 343–351. DOI: 10.1016/j.chemgeo.2010.12.020.

Vlastélic, I., A. Di Muro, P. Bachèlery, L. Gurioli, D. Auclair, and A. Gannoun (2018). "Control of source fertility on the eruptive activity of Piton de la Fournaise volcano, La Réunion". *Scientific Reports* 8(1). DOI: 10.1038/s41598-018-32809-0.

Wadge, G. (1980). "Output rate of magma from active central volcanoes". *Nature* 288(5788), pages 253–255. DOI: 10.1038/288253a0.

– (1982). "Steady state volcanism: Evidence from eruption histories of polygenetic volcanoes". *Journal of Geophysical Research: Solid Earth* 87(B5), pages 4035–4049. DOI: 10.1029/jb087ib05p04035.

Wadge, G. and J. E. Guest (1981). "Steady-state magma discharge at Etna 1971–81". *Nature* 294(5841), pages 548–550. DOI: 10.1038/294548a0.

Walker, A. M. (1969). "On the Asymptotic Behaviour of Posterior Distributions". *Journal of the Royal Statistical Society Series B: Statistical Methodology* 31(1), pages 80–88. DOI: 10.1111/j.2517-6161.1969.tb00767.x.

Wauthier, C., V. Cayol, B. Smets, N. D'Oreye, and F. Kervyn (2015). "Magma Pathways and Their Interactions Inferred from InSAR and Stress Modeling at Nyamulagira Volcano, D.R. Congo". *Remote Sensing* 7(11), pages 15179–15202. DOI: 10.3390/rs71115179.

White, S. M., J. A. Crisp, and F. J. Spera (2006). "Long-term volumetric eruption rates and magma budgets". *Geochemistry, Geophysics, Geosystems* 7(3). DOI: 10.1029/2005gc001002.

Williams, R. and J. Moore (1976). *Man against volcano: The eruption on Heimaey, Vestmann Islands, Iceland*. DOI: 10.3133/70039211.

Wolfe, E. W., editor (1988). *The Puu Oo eruption of Kilauea Volcano, Hawaii: Episodes 1 through 20, January 3, 1983, through June 8, 1984*. DOI: 10.3133/pp1463. Professional Paper 1463.

Wright, T. L. and F. W. Klein (2014). *Two hundred years of magma transport and storage at Kīlauea Volcano, Hawai'i, 1790–2008*. U.S. Geological Survey. 240 pages. DOI: 10.3133/pp1806. U.S. Geological Survey Professional Paper 1806.

Xu, W., S. Jónsson, J. Ruch, and Y. Aoki (2016). "The 2015 Wolf volcano (Galápagos) eruption studied using Sentinel-1 and ALOS-2 data". *Geophysical Research Letters* 43(18), pages 9573–9580. DOI: 10.1002/2016gl069820.

Xu, W., L. Xie, R. Bürgmann, X. Liu, and J. Wang (2023). "The 2022 Eruption of Wolf Volcano, Galápagos: The Role of Caldera Ring-Faults During Magma Transfer From InSAR Deformation Data". *Geophysical Research Letters* 50(14). DOI: 10.1029/2023gl103704.

Yamamoto, T., T. Kudo, and O. Isizuka (2018). "Temporal variations in volumetric magma eruption rates of Quaternary volcanoes in Japan". *Earth, Planets and Space* 70(1). DOI: 10.1186/s40623-018-0849-x.